

inhibits HA synthesis of group C *Streptococcus* in a cardiolipin-dependent fashion without significant change in HAS activity in the cell-free HA system. The discrepancy between this result and the observations reported in this paper may be due to a different level of MU-GlcUA in the *Streptococcus*. Indeed, the production of MU-GlcUA was not detected in either the conditioned medium or in the cell extract of *Streptococcus*. Furthermore, the effect of cardiolipin on enzymatic activity is distinct between mammalian HAS and streptococcal HAS (29). Although the mechanism of action of MU is complex, our results suggest that glucuronidation of MU partially accounts for the inhibition of HA synthesis in mammalian cells.

Specific inhibitors targeting HA biosynthesis may serve as useful drugs to prevent the malignant alteration of cancer or the fibrosis of organs. Clinical application of MU, based on the inhibition of HA synthesis, is feasible because this compound has been used safely for many years as a cholagogue in human medicine (27). Nevertheless, it is important to avoid the use of a very high dose of MU thereby reducing the possibility of cytotoxicity. The information presented in this report will be useful in the development of new drugs with improved efficacy. In particular, other acceptors for UGTs should be potent inhibitors of HAS activity. Further investigation will be undertaken in this regard.

**Acknowledgments**—We thank Drs. Andrew P. Spicer (Texas A and M University) and John A. McDonald (University of Utah) for providing mouse HAS2 cDNA. We also thank Dr. Minoru Okayama (Kyoto Sangyo University, Kyoto, Japan) for helpful comments.

## REFERENCES

- Laurent, T. C., and Fraser, J. R. E. (1992) *FASEB J.* **6**, 2397–2404
- Knudson, C. B., and Knudson, W. (1993) *FASEB J.* **7**, 1233–1241
- Knudson, W., Biswas, C., Li, X. Q., Nemecek, R. E., and Toole, B. P. (1989) *CIBA Found. Symp.* **143**, 150–159
- Toole, B. P., Wight, T. N., and Tammi, M. I. (2002) *J. Biol. Chem.* **277**, 4593–4596
- Laurent, T. C., Laurent, U. B., and Fraser, J. R. (1996) *Ann. Med.* **28**, 241–253
- Levesque, H., Girard, N., Maingonnat, C., Delpech, A., Chauzy, C., Tayot, J., Courtois, H., and Delpech, B. (1994) *Atherosclerosis* **105**, 51–62
- Satoh, T., Ichida, T., Matsuda, Y., Sugiyama, M., Yonekura, K., Ishikawa, T., and Asakura, H. (2000) *J. Gastroenterol. Hepatol.* **15**, 402–411
- Plebani, M., and Burlina, A. (1991) *Clin. Biochem.* **24**, 219–239
- El Maradny, E., Kanayama, N., Kobayashi, H., Hossain, B., Khatun, S., Liping, S., Kobayashi, T., and Terao, T. (1997) *Hum. Reprod.* **12**, 1080–1088
- Kosaki, R., Watanabe, K., and Yamaguchi, Y. (1999) *Cancer Res.* **59**, 1141–1145
- Itano, N., Sawai, T., Miyaishi, O., and Kimata, K. (1999) *Cancer Res.* **59**, 2499–2504
- Liu, N., Gao, F., Han, Z., Xu, X., Underhill, C. B., and Zhang, L. (2001) *Cancer Res.* **61**, 5207–5214
- Simpson, M. A., Wilson, C. M., Furcht, L. T., Spicer, A. P., Oegema, T. R., Jr., and McCarthy, J. B. (2002) *J. Biol. Chem.* **277**, 10050–10057
- Jacobson, A., Rahmanian, M., Rubin, K., and Heldin, P. (2002) *Int. J. Cancer* **102**, 212–219
- Weissman, B., and Meyer, K. (1954) *J. Am. Chem. Soc.* **76**, 1753–1757
- Tammi, M. I., Day, A. J., and Turley, E. A. (2002) *J. Biol. Chem.* **277**, 4581–4584
- Weigel, P. H., Hascall, V. C., and Tammi, M. (1997) *J. Biol. Chem.* **272**, 13997–14000
- Goldberg, R. L., and Toole, B. P. (1983) *J. Biol. Chem.* **258**, 7041–7046
- Smith, T. J. (1990) *J. Clin. Endocrinol. Metab.* **70**, 655–660
- Zaharevitz, D. W., Chisena, C. A., Duncan, K. L., August, E. M., and Cysyk, R. L. (1993) *Biochem. Mol. Biol. Int.* **31**, 627–633
- August, E. M., Duncan, K. L., Malinowski, N. M., and Cysyk, R. L. (1993) *Oncol. Res.* **5**, 415–422
- Ueki, N., Taguchi, T., Takahashi, M., Adachi, M., Ohkawa, T., Amuro, Y., Hada, T., and Higashino, K. (2000) *Biochim. Biophys. Acta* **1495**, 160–167
- Nakamura, T., Takagaki, K., Shibata, S., Tanaka, K., Higuchi, T., and Endo, M. (1995) *Biochem. Biophys. Res. Commun.* **208**, 470–475
- Nakamura, T., Funahashi, M., Takagaki, K., Munakata, H., Tanaka, K., Saito, Y., and Endo, M. (1997) *Biochem. Mol. Biol. Int.* **43**, 263–268
- Endo, Y., Takagaki, K., Takahashi, G., Kakizaki, I., Funahashi, M., Yokoyama, M., and Endo, M. (2000) in *Progress in Transplantation* (Munakata, A., ed) pp. 1–7, Elsevier Science Publishers B. V., Amsterdam
- Sohara, Y., Ishiguro, N., Machida, K., Kurata, H., Thant, A. A., Senga, T., Matsuda, S., Kimata, K., Iwata, H., and Hamaguchi, M. (2001) *Mol. Biol. Cell* **12**, 1859–1868
- Takeda, S., and Aburada, M. (1981) *J. Pharmacobiodyn.* **4**, 724–734
- Kakizaki, I., Takagaki, K., Endo, Y., Kudo, D., Ikeya, H., Miyoshi, T., Baggenstoss, B. A., Tlapak-Simmons V. L., Kumari, K., Nakane, A., Weigel, P. H., and Endo, M. (2002) *Eur. J. Biochem.* **269**, 5066–5075
- Yoshida, M., Itano, N., Yamada, Y., and Kimata, K. (2000) *J. Biol. Chem.* **275**, 497–506
- Chichibu, K., Matsuura, T., Shichijo, S., and Yokoyama, M. M. (1989) *Clin. Chim. Acta* **181**, 317–323
- Ito, M., Yamamoto, K., Maruo, Y., Sato, H., Fujiyama, Y., and Bamba, T. (2002) *Eur. J. Clin. Pharmacol.* **58**, 11–14
- Itano, N., Sawai, T., Yoshida, M., Lenas, P., Yamada, Y., Imagawa, M., Shinomura, T., Hamaguchi, M., Yoshida, Y., Ohnuki, Y., Miyauchi, S., Spicer, A. P., McDonald, J. A., and Kimata, K. (1999) *J. Biol. Chem.* **274**, 25085–25092
- Knudson, W., and Knudson, C. B. (1991) *J. Cell Sci.* **99**, 227–235
- Zimmerman, C. L., Ratna, S., Leboeuf, E., and Pang, K. S. (1991) *J. Chromatogr.* **563**, 83–94
- Kamst, E., Bakkers, J., Quaedvlieg, N. E., Pilling, J., Kijne, J. W., Lugtenberg, B. J., and Spalink, H. P. (1999) *Biochemistry* **38**, 4045–4052
- Kanou, M., Saeki, K., Kato, T., Takahashi, K., Mizutani, T. (2002) *Fundam. Clin. Pharmacol.* **16**, 513–517
- Takagaki, K., Kojima, K., Majima, M., Nakamura, T., Kato, I., and Endo, M. (1992) *Glycoconj. J.* **9**, 174–179
- Hanioka, N., Jinno, H., Tanaka-Kagawa, T., Nishimura, T., and Ando, M. (2001) *J. Pharm. Biomed. Anal.* **25**, 65–75
- Ciotti, M., Marrone, A., Potter, C., and Owens, I. S. (1997) *Pharmacogenetics* **7**, 485–495
- Bock-Hennig, B. S., Kohle, C., Nill, K., and Bock, K. W. (2002) *Biochem. Pharmacol.* **63**, 123–128
- Sobue, M., Habuchi, H., Ito, K., Yonekura, H., Oguri, K., Sakurai, K., Kamohara, S., Ueno, Y., Noyori, R., and Suzuki, S. (1987) *Biochem. J.* **241**, 591–601
- Takagaki, K., Nakamura, T., Kon, A., Tamura, S., and Endo, M. (1991) *J. Biochem. (Tokyo)* **109**, 514–519
- Matuoka, K., Mitsui, Y., and Murota, S. (1985) *Cell Biol. Int. Rep.* **9**, 577–586
- Itano, N., Sawai, T., Atsumi, F., Miyaishi, O., Taniguchi, S., Kannagi, R., Hamaguchi, M., and Kimata, K. (2004) *J. Biol. Chem.* **279**, 18679–18687
- Peng, L., Kawagoe, Y., Hogan, P., and Delmer, D. (2002) *Science* **295**, 147–150
- Gressner, A. M. (1991) *Exp. Mol. Pathol.* **55**, 143–169
- Gressner, A. M. (1991) *Biochem. Pharmacol.* **42**, 1987–1995
- McCormick, C., Leduc, Y., Martindale, D., Mattison, K., Esford, L. E., Dyer, A. P., and Tufaro, F. (1998) *Nat. Genet.* **19**, 158–161
- Lind, T., Tufaro, F., McCormick, C., Lindahl, U., and Lidholt, K. (1998) *J. Biol. Chem.* **273**, 26265–26268
- Kitagawa, H., Uyama, T., and Sugahara, K. (2001) *J. Biol. Chem.* **276**, 38721–38726
- Yada, T., Gotoh, M., Sato, T., Shionyu, M., Go, M., Kaseyama, H., Iwasaki, H., Kikuchi, N., Kwon, Y. D., Togayachi, A., Kudo, T., Watanabe, H., Narimatsu, H., and Kimata, K. (2003) *J. Biol. Chem.* **278**, 30235–30247
- Yada, T., Sato, T., Kaseyama, H., Gotoh, M., Iwasaki, H., Kikuchi, N., Kwon, Y. D., Togayachi, A., Kudo, T., Watanabe, H., Narimatsu, H., and Kimata, K. (2003) *J. Biol. Chem.* **278**, 39711–39725
- Radomska-Pandya, A., Pokrovskaya, I. D., Xu, J., Little, J. M., Jude, A. R., Kurten, R. C., and Czernik, P. J. (2002) *Arch. Biochem. Biophys.* **399**, 37–48
- Ouzzine, M., Antonio, L., Burchell, B., Netter, P., Fournel-Gigleux, S., and Magdalou, J. (2000) *Mol. Pharmacol.* **58**, 1609–1615

## *In Vivo* Hyaluronan Synthesis upon Expression of the Mammalian Hyaluronan Synthase Gene in *Drosophila*\*

Received for publication, December 30, 2003, and in revised form, February 9, 2004  
Published, JBC Papers in Press, February 13, 2004, DOI 10.1074/jbc.M314293200

Satomi Takeo‡, Momoko Fujise§, Takuya Akiyama¶, Hiroko Habuchi§, Naoki Itano§,  
Takashi Matsuo‡, Toshiro Aigaki‡, Koji Kimata§, and Hiroshi Nakato¶

From the ‡Department of Biological Sciences, Tokyo Metropolitan University, Hachioji-shi, Tokyo 192-0397, Japan, the §Institute for Molecular Science of Medicine, Aichi Medical University, Nagakute, Aichi 480-1195, Japan, and the ¶Department of Genetics, Cell Biology, and Development, University of Minnesota, Minneapolis, Minnesota 55455

Hyaluronan (HA) is a large linear polymer of repeating disaccharides of glucuronic acid and GlcNAc. Although HA is widely distributed in vertebrate animals, it has not been found in invertebrates, including insect species. Insects utilize chitin, a repeating  $\beta$ -1,4-linked homopolymer of GlcNAc, as a major component of their exoskeleton. Recent studies illustrate the similarities in the biosynthetic mechanisms of HA and chitin and suggest that HA synthase (HAS) and chitin synthase have evolved from a common ancestral molecule. Although the biochemical properties and *in vivo* functions of HAS proteins have been extensively studied, the molecular basis for HA biosynthesis is not completely understood. For example, it is currently not clear if proper chain elongation and secretion of HA require other components in addition to HAS. Here, we demonstrate that a non-HA-synthesizing animal, the fruit fly *Drosophila melanogaster*, can produce HA *in vivo* when a single HAS protein is introduced. Expression of the mouse *HAS2* gene in *Drosophila* tissues by the Gal4/UAS (upstream activating sequence) system resulted in massive HA accumulation in the extracellular space and caused various morphological defects. These morphological abnormalities were ascribed to disordered cell-cell communications due to accumulation of HA rather than disruption of heparan sulfate synthesis. We also show that adult wings with HA can hold a high level of water. These findings demonstrate that organisms synthesizing chitin (but not HA) are capable of producing HA that is structurally and functionally relevant to that in mammals. The ability of insect cells to produce HA supports the idea that *in vivo* HA biosynthesis does not require molecules other than the HAS protein. An alternative model is that *Drosophila* cells use endogenous components of the chitin biosynthetic machinery to produce and secrete HA.

Polysaccharides are used as major structural components of animal and plant bodies. In higher vertebrates, hyaluronan (HA),<sup>1</sup> a high molecular mass glycosaminoglycan composed of

repeating  $\beta$ -1,4-linked disaccharides of glucuronic acid (GlcUA) and  $\beta$ -1,3-linked GlcNAc, is found in the extracellular matrix in many tissues, including cartilage, synovial joint, and the vitreous of the eye (1). Despite wide distribution of HA in vertebrate animals, HA has not been found in invertebrates such as arthropod species. Instead of HA, crustaceans and arthropods produce chitin, a repeating  $\beta$ -1,4-linked homopolymer of GlcNAc, and deposit it in their exoskeleton. In addition, the plant cell wall is composed mainly of cellulose,  $\beta$ -1,4-glucan. These distinct types of polysaccharides share common important functions to determine and maintain the basic architecture of organisms, suggesting an evolutionarily conserved role of the polysaccharides as major structural constituents of multicellular organisms. Consistent with this idea, the biosynthetic mechanisms of these molecules show some intriguing similarities. All enzymes that synthesize HA, chitin, and cellulose are integral plasma membrane proteins and have the invariant amino acid residues QXXRW in their catalytic domains (2). Interestingly, one of the HA synthases (HASs), mouse HAS1, is indeed capable of synthesizing chito-oligosaccharides *in vitro* when only UDP-GlcNAc is supplied as substrate in the system (2). Based on these similarities, it has been proposed that three classes of glycosyltransferases (HASs, chitin synthases, and cellulose synthases) diverged from a common ancestral molecule.

HA is a multifunctional player in the vertebrate extracellular matrix. One of the important features of the HA network is its ability to hold a large amount of water, exhibiting viscoelastic properties. HA also directly affects cell behavior through its cell-surface receptors: CD44 (for review, see Ref. 3), RHAMM (receptor for HA-mediated motility) (4, 5), and Layilin (6). Recent studies on HASs, including molecular cloning of HAS cDNAs (7–13) and genes (14, 15) and functional analyses of each HAS gene (2, 16–20), illustrate the biological importance of HA. However, little is known about the mechanism of HA synthesis. Membrane extracts prepared from yeast cells expressing the *Xenopus HAS (DG42)* gene showed HA synthesizing activity *in vitro* solely in the presence of exogenously supplied substrates and magnesium ions (21). Furthermore, a purified single HAS1 protein or a *HAS1* gene product of an *in vitro* transcription/translation system has been shown to have HAS activity (2). These results indicate that the HAS protein alone can synthesize HA *in vitro* without any other protein factors. However, it is not clear whether other components are required for *in vivo* HA biosynthesis for proper chain elongation, termination, and secretion.

In this study, we demonstrate that a single mammalian HAS

\* This work was supported in part by National Institutes of Health Grant HD042769 and Human Frontier Science Program Grant RGP0009/2003. The costs of publication of this article were defrayed in part by the payment of page charges. This article must therefore be hereby marked "advertisement" in accordance with 18 U.S.C. Section 1734 solely to indicate this fact.

¶ To whom correspondence should be addressed: Dept. of Genetics, Cell Biology, and Development, University of Minnesota, 6-160 Jackson Hall, 321 Church St. SE., Minneapolis, MN 55455. Tel.: 612-625-1727; Fax: 612-626-5652; E-mail: nakat003@umn.edu.

<sup>1</sup> The abbreviations used are: HA, hyaluronan; GlcUA, glucuronic

acid; HAS, hyaluronan synthase; UAS, upstream activating sequence; b-HABP, biotinylated HA-binding protein.

protein (HAS2) can efficiently synthesize and secrete HA in *Drosophila*, which is a chitin-synthesizing organism and which does not naturally produce HA. This implies that conversion of the biosynthetic machinery of chitin to that of HA can happen by a single molecule exchange: substitution of chitin synthase with HAS. HAS2 expression caused various morphological defects due to disruption of cell-cell communication. HA synthesized in fly tissues was able to retain a high level of water, which is the characteristic biophysical feature of this macromolecule. The ability of *Drosophila* cells to produce functional HA supports the idea that HAS is the only critical factor required for normal HA biosynthesis. Another interesting possibility is that HA is produced by HAS together with endogenous components involved in chitin biosynthesis.

#### EXPERIMENTAL PROCEDURES

**Upstream Activating Sequence (UAS) Constructs and Ectopic Expression**—The UAS-HAS2 transgene was constructed by cloning the full-length mouse HAS2 cDNA into the pUAST vector. Transgenic flies were obtained by P-element-mediated germ line transformation (22). In this study, we used two independent HAS2 transgenic strains (UAS-HAS2-1 and UAS-HAS2-2) that bear transgenic insertions at different chromosomal locations. The HAS2 gene was misexpressed in the Gal4/UAS system (23) using the following Gal4 drivers. 29BD-GAL4 is an enhancer trap line of P(GawB) and ubiquitously expresses a high level of Gal4 protein (24). engrailed-GAL4 and apterous-GAL4 were used to express HAS2 in the posterior and dorsal compartments of the wing disc, respectively. GMR-GAL4 and A9-GAL4 drive target gene expression in developing eyes and wings, respectively. To overexpress *sugarless* (*sgl*), we used the transgenic strain bearing the *sgl* gene under the control of the ubiquitin promoter (*ubi-sgl*) (25).

**Preparation and Quantification of Glycosaminoglycans**—To quantify HA and chondroitin sulfate, crude glycosaminoglycans from 25 mg of lyophilized *Drosophila* third instar larvae were prepared as described previously (26) and dissolved in 100  $\mu$ l of H<sub>2</sub>O. A 20- $\mu$ l portion of the crude glycosaminoglycans was digested with 2 turbidity reducing unit of *Streptomyces* hyaluronidase in 100  $\mu$ l of 50 mM acetate buffer (pH 6.0) at 60 °C for 1 h. The resulting hyaluronic acid tetrakis- and hexasaccharides were then filtered with Ultrafree-MC (5000 nominal molecular weight limit). HA contained in the filtrates and the recovered glycosaminoglycans retained on the filter were digested separately with chondroitinases ABC and ACII and 5  $\mu$ g of bovine serum albumin in 50  $\mu$ l of 50 mM Tris-HCl (pH 8) at 37 °C for 2 h. The digests were filtered with Ultrafree-MC (5000 nominal molecular weight limit), and unsaturated disaccharides contained in the filtrates were determined by reversed-phase ion pair chromatography using a Senshu-Pak Docosil column equipped with a post-column fluorescence detector according to the method of Toyoda *et al.* (26) except for a slight modification of the elution conditions.

For preparation and quantification of heparan sulfate, a 10- $\mu$ l portion of the crude glycosaminoglycans was digested with a mixture of 10 milliunits of heparitinase I, 5 milliunits of heparitinase II, and 10 milliunits of heparitinase III in 50  $\mu$ l of 50 mM Tris-HCl (pH 7.2), 1 mM CaCl<sub>2</sub>, and 4  $\mu$ g of bovine serum albumin at 37 °C for 16 h. The digests were analyzed as described above.

**Preparation and Quantification of Chitin**—For the quantitative measurement of chitin, the amount of GlcNAc released by chitinase was measured by a colorimetric method. Lyophilized *Drosophila* larvae (25 mg, dry weight) were homogenized with 1.0 ml of acetone. The homogenate was washed with acetone and dried. The pellet was suspended in 1.0 ml of 0.1 N NaOH for 16 h at room temperature. After alkali treatment, 25  $\mu$ l of 4 N acetic acid were added; actinase E was then added and incubated at 37 °C for 2 h. Insoluble material was isolated by centrifugation, washed twice with water, and resuspended in 400  $\mu$ l of 200 mM acetate buffer (pH 5.0). Chitinase (2.0 mg) from *Bacillus* sp. dissolved in the same buffer (200 mM) was added, and the mixed solution was incubated at 37 °C for 90 min. After centrifugation, an 80- $\mu$ l aliquot of each sample was assayed for GlcNAc by measuring the absorbance at 585 nm (27).

**Agarose Gel Electrophoresis of HA**—A 20- $\mu$ l portion of the crude glycosaminoglycans prepared as described above was fractionated by 0.5% agarose gel electrophoresis (28). After electrophoresis, HA was blotted onto nylon membrane and detected by the ECL detection system with biotinylated HA-binding protein (b-HABP) (Seikagaku Co.) as a probe as described previously (17). HA with average masses of 21.3,

14.1, 9.9, 6.4, 4.6, and 1.0  $\times$  10<sup>5</sup> Da was used as a standard.

To test the sensitivity of detected bands to chitinase and hyaluronidase, the crude glycosaminoglycan fractions were treated with these enzymes before gel electrophoresis. The samples were incubated with 0.5 mg of chitinase from *Bacillus* sp. at 37 °C for 90 min (29). After inactivation of chitinase by heating at 95 °C for 5 min, glycosaminoglycans were recovered by ethanol precipitation. Subsequently, the samples were incubated with or without 0.1 turbidity reducing unit of *Streptomyces* hyaluronidase at 55 °C for 1 h.

**Histochemical Staining**—To detect HA *in situ* in *Drosophila* tissues, histochemical staining was performed using b-HABP as a probe (17). Wing imaginal discs were dissected from third instar larvae and fixed with 4% formaldehyde in phosphate-buffered saline for 50 min. Endogenous peroxidase activity was quenched with 0.3% H<sub>2</sub>O<sub>2</sub> in methanol. After washing with 0.3% Triton X-100 in phosphate-buffered saline, nonspecific binding was blocked with 10% goat serum in 0.3% Triton X-100 in phosphate-buffered saline. The discs were incubated with 2.5  $\mu$ g/ml b-HABP in 10% goat serum overnight at 4 °C. After unbound probe was washed off, the discs were incubated with Avidin-Biotin Complex reagent (Vector Labs, Inc.) for 1 h, and b-HABP was detected by staining with 0.5 mg/ml 3,3'-diaminobenzidine and 0.03% H<sub>2</sub>O<sub>2</sub> diluted in phosphate-buffered saline. For subcellular localization of HA, the signal was amplified and detected using a tyramide signal amplification fluorescence system (PerkinElmer Life Sciences) and imaged using an LSM410 confocal microscope (Carl Zeiss, Inc.). Cobalt sulfide staining was performed to visualize the apical surface of pupal retina as described previously (30).

**Quantification of the H<sub>2</sub>O Content of *Drosophila* Adult Wings**—Adult wings were collected from wild-type or 29BD-GAL4/UAS-HAS2-2 males at 3–5 days after eclosion. To prevent evaporation of water from the tissue, wings were rapidly removed from the thorax at the base using forceps. Approximately 25–50 wings (0.1–0.2 mg) were used as a sample to measure the H<sub>2</sub>O content by the coulometric Karl-Fischer method (31, 32) using an AQ-6 water content analyzer (Hiranuma Sangyo Co.). Immediately after the fresh weight of each sample was determined using an S4 Ultramicro balance (Sartorius Corp.), water was extracted from the wings and titrated with Hydranal Aqualyte RS (Riedel-deHaen Co.) as a titrant. Aqualyte CN (Kanto Kagaku Co.) was used as a solvent. Sets of four and six samples were prepared for wild-type and 29BD-GAL4/UAS-HAS2-2 wings, respectively, and measurements were performed independently.

#### RESULTS

**HA Synthesis upon HAS2 Expression in *Drosophila***—A previous biochemical study on glycosaminoglycans from *Drosophila* showed that no detectable HA exists in this organism (26). We first asked whether *Drosophila* cells have the ability to synthesize HA when a HAS protein is introduced. We used the Gal4/UAS system (23) to drive expression of the mouse HAS2 gene *in vivo*. The HAS2 cDNA was ligated downstream of the UAS, and the resultant plasmid construct was integrated into the genomic DNA by P-element-mediated transformation. The established *Drosophila* strains bearing the UAS-HAS2 transgene were crossed with various Gal4 strains to express HAS genes ubiquitously or in a tissue-specific manner. To determine whether HA is synthesized in the HAS gene-expressing animals, we prepared crude glycosaminoglycan fractions from third instar larvae according to the method described previously (26) and quantified HA. A large amount of HA was detected in larvae obtained from crosses between the 29BD-GAL4 driver and two independent UAS-HAS2 transgenic strains, whereas no detectable HA was observed in the wild-type control animals (Table I).

We also examined HA synthesis *in situ* using b-HABP as a probe. HAS2 expression was induced by engrailed-GAL4, which drives Gal4 expression in the posterior compartment of imaginal discs (Fig. 1A). Histochemical staining showed specific binding of the b-HABP probe to the posterior half of the wing (Fig. 1B). This result confirmed that HA is synthesized in *Drosophila* tissues and accumulates at the sites of HAS2 expression. We also used this probe in a fluorescence detection system to determine the subcellular localization of HA. As shown in Fig. 1C, signals were detected mainly on the cell

TABLE I  
Determination of the amounts of glycosaminoglycans and chitin from *HAS2*-transgenic *Drosophila*

Crude glycosaminoglycans were prepared from wild-type and *29BD**HAS2* third instar larvae. The amounts of HA, chondroitin sulfate (CS), and heparan sulfate (HS) were determined by fluorescence disaccharide analysis. Chitin was also quantified as described under "Experimental Procedures." Two independent transgenic strains for *UAS-HAS2* (*UAS-HAS2-1* and *UAS-HAS2-2*) were used for this analysis. ND, not detectable.

Genotype	HA	CS	HS	Chitin
	nmol/mg (dry weight)	nmol/mg (dry weight)	nmol/mg (dry weight)	pmol/mg (dry weight)
Wild-type	ND	0.54	0.14	5.8
<i>29BD</i> <i>HAS2-1</i>	0.20	0.54	0.10	5.6
<i>29BD</i> <i>HAS2-2</i>	0.04	0.56	0.14	5.4

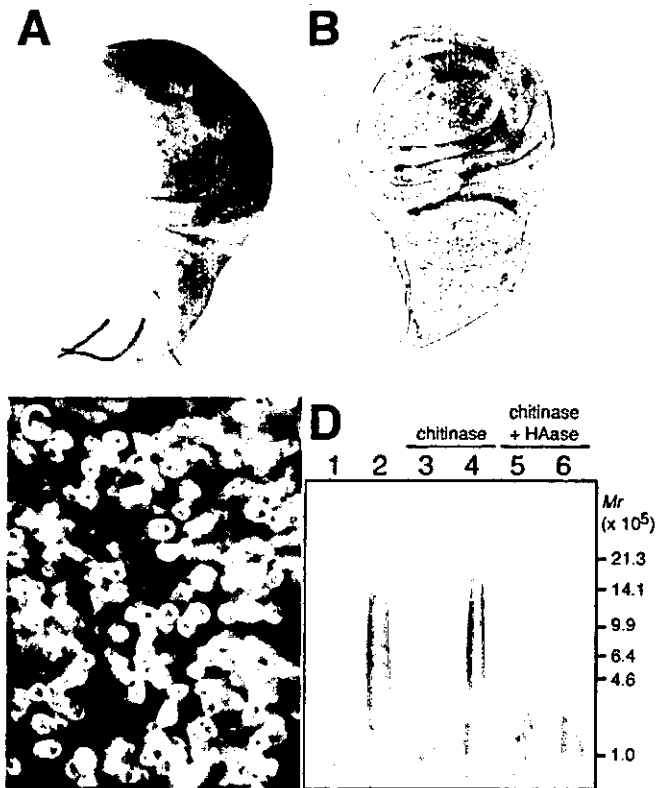


Fig. 1. HA synthesis upon mouse *HAS2* expression in *Drosophila* wing discs. **A**, the posterior compartment-specific pattern of *engrailed-GAL4* expression in the wing disc. The expression pattern of *lacZ* in *engrailed-GAL4/UAS-lacZ* wing discs was monitored by  $\beta$ -galactosidase activity staining. **B**, HA localization in the *engrailed-GAL4/UAS-HAS2-2* wing disc determined by staining using b-HABP as a probe. HA was specifically detected in the posterior region where *HAS2* was overexpressed by *engrailed-GAL4*. **C**, subcellular localization of HA in the *HAS2*-expressing disc. The fluorescent signal of HA was detected on the cell surface and/or in the extracellular space. **D**, agarose gel electrophoresis of HA synthesized in *Drosophila*. Crude glycosaminoglycan fractions were prepared from wild-type (lanes 1, 3, and 5) and *29BD-GAL4/UAS-HAS2-2* (lanes 2, 4, and 6) animals as described under "Experimental Procedures" and separated by agarose gel electrophoresis. Samples loaded in lanes 3 and 4 were treated with chitinase (from *Bacillus* sp.) before gel electrophoresis; those loaded in lanes 5 and 6 were digested with both chitinase and *Streptomyces* hyaluronidase (HAase). HA was blotted onto nylon membrane and detected using the ECL detection system with b-HABP as a probe. HA with average masses of 21.3, 14.1, 9.9, 6.4, 4.6, and  $1.0 \times 10^5$  Da was used as a standard.

surface, suggesting that synthesized HA is secreted and deposited on the cell surface or in the extracellular matrix.

We next analyzed the size distribution of HA synthesized in the *HAS2* transgenic animals. Crude glycosaminoglycan fractions prepared from wild-type and *29BD-GAL4/UAS-HAS2* larvae were separated by agarose gel electrophoresis. HA was blotted onto nylon membrane and detected using b-HABP as a probe. In the crude glycosaminoglycan preparation from *HAS2*-expressing animals, we detected HA, which migrated as broad

peaks with large molecular masses ranging from  $1 \times 10^5$  to  $2 \times 10^6$  Da (Fig. 1D, lane 2). The size distribution of HA prepared from *29BD-GAL4/UAS-HAS2* animals was smaller than that synthesized by the same enzyme in rat 3Y1 fibroblasts (molecular masses of  $>2 \times 10^6$  Da), but was comparable with that produced *in vitro* by membrane preparation of *HAS2* transfectant (molecular masses of  $2 \times 10^5$  to  $2 \times 10^6$  Da) (17). On the other hand, a weak background signal was observed at a low molecular mass range in the wild-type control lane (Fig. 1D, lane 1). To determine whether this low molecular mass smear band reflects the existence of HA or other related molecules in the wild-type fraction, we tested its sensitivity to chitinase (*Bacillus*) and hyaluronidase (*Streptomyces*). As shown in lanes 3 and 5, the low molecular mass signals were not eliminated by incubation with chitinase or hyaluronidase, indicating that these signals do not represent either HA or chitin. In contrast, HA produced in *HAS2*-expressing animals was not affected by chitinase treatment (lane 4), but was completely degraded by adding hyaluronidase (lane 6). Although the nature of the low molecular mass band is unknown, it seems to be a background signal detectable only in blotting experiments because the b-HABP probe specifically recognized regions of the wing discs where *HAS2* was expressed *in situ* (Fig. 1B) and did not stain wild-type discs (data not shown).

***HAS2* Gene Expression Disrupts Morphogenesis in *Drosophila* Tissues**—Overexpression of *HAS2* using several different Gal4 drivers caused lethality and a variety of morphological defects in adult tissues (Fig. 2). Eye-specific expression of the *HAS2* gene by *GMR-GAL4* induced a so-called "rough eye" phenotype, characterized by reduced numbers of ommatidia and disordered ommatidial arrays of the compound eye (Fig. 2B). To further analyze this eye defect, we observed pupal retina stained with cobalt sulfide (Fig. 2, C and D). In contrast to wild-type retina, which showed precise and ordered patterns of differentiation of ommatidial components, *HAS2*-expressing eyes exhibited several distinct defects. These abnormalities included decreased numbers of cone cells, abnormal sizes and shapes of primary pigment cells, and ectopic interommatidial bristles. Overexpression of *HAS2* in the developing wing using *A9-GAL4* led to thickened and disarranged wing veins (Fig. 2, E and F). When *HAS2* expression was induced in the dorsal part of wing imaginal discs by *apterous-GAL4*, the wings failed to extend. In addition, the patterns and formation of notal bristles were disrupted; most large mechanosensory bristles (macrochaetae) were lost or shortened with abruptly ended tips (Fig. 2, G and H). In this study, we used two independent *HAS2* transgenic strains, *UAS-HAS2-1* and *UAS-HAS2-2*. The phenotypes associated with *HAS2* expression by these two transgenes were fundamentally similar, but different in severity (Table II). Expression of *UAS-HAS2-1*, which produces higher levels of HA, resulted in more severe expressivity and higher penetrance compared with that of *UAS-HAS2-2*.

All these abnormalities are known to be caused by defective intercellular signaling. For example, during eye development, differentiation of cone and pigment cells requires activation of the *Drosophila* epidermal growth factor receptor (DER), and

# Differential Regulation by IL-1 $\beta$ and EGF of Expression of Three Different Hyaluronan Synthases in Oral Mucosal Epithelial Cells and Fibroblasts and Dermal Fibroblasts: Quantitative Analysis Using Real-Time RT-PCR

Yoichi Yamada,\*† Naoki Itano,† Ken-ichiro Hata,\* Minoru Ueda,† and Koji Kimata†

\*Center for Genetic and Regenerative Medicine, Nagoya University School of Medicine, Nagoya, Japan; †Institute for Molecular Science of Medicine, Aichi Medical University, Aichi, Japan; ‡Department of Oral and Maxillofacial Surgery, Nagoya University Graduate School of Medicine, Nagoya, Japan

Using "real-time RT-PCR", we assessed the expression of three different hyaluronan synthase genes, *HAS1*, *HAS2*, and *HAS3*, by measuring their mRNA amounts in cultured human oral mucosal epithelial (COME) cells, oral mucosal fibroblasts, and dermal fibroblasts, and investigated the effects of interleukin-1 $\beta$  (IL-1 $\beta$ ) and epidermal growth factor (EGF). When COME cells were treated with IL-1 $\beta$  or EGF, early and marked increases and subsequent rapid decreases were observed for all HAS genes and, moreover, actual changes in hyaluronan synthesis subsequently occurred. The effects of IL-1 $\beta$  stimulation were concentration-dependent and the maximal response to the EGF stimulation was observed at a low concentration (0.1 ng per mL). When two different types of fibroblasts were treated with IL-1 $\beta$  or EGF, increased expression with different degrees and rates of three different HAS genes and subsequent increased synthesis of hyaluronan were also observed. In addition, *HAS1* gene expression was not detectable in the mucosal fibroblasts, while weak *HAS3* gene expression was detected in the dermal fibroblasts. Taken together, it is likely that the regulation of the expression of the three different HAS genes is different between oral mucosa and skin, which may be of significance for elucidating some of the differences between these tissues in wound healing.

Key words: hyaluronan/hyaluronan synthase genes/real-time RT-PCR analysis/tissue engineering  
J Invest Dermatol 122:631–639, 2004

The process of wound healing depends upon a variety of interactions between cells and the extracellular matrix (Clark and Henson, 1988). It is well known that hyaluronan not only supports tissue architecture as a passive structural component of the matrix in various connective tissues but is also involved in dynamic cellular processes such as cell migration and cell–cell recognition during wound healing and inflammation (Weigel *et al*, 1997; Knudson *et al*, 1989; Turley, 1989). Three different mammalian hyaluronan synthases, *HAS1*, *HAS2*, and *HAS3*, have been identified and characterized (Rosa *et al*, 1988; Itano and Kimata, 1996a,b; Shyjan *et al*, 1996; Spicer *et al*, 1996; Watanabe and Yamaguchi, 1996; Spicer *et al*, 1997). The three HAS genes show distinct expression patterns (Spicer and McDonald, 1998) and the synthases are significantly different in their enzymatic properties and in their role in the pericellular hyaluronan coat formation (Itano *et al*, 1999). The precise regulatory mechanism of the expression of each HAS is still unknown. It has been shown that the

synthesis of hyaluronan is stimulated by some growth regulatory factors and anti-inflammatory cytokines such as epidermal growth factor (EGF) and IL-1 $\beta$  (Heldin *et al*, 1989; Yung *et al*, 1996; Kaback and Smith, 1999), which have also been shown to be agents that promote wound healing (Brown *et al*, 1986; Gailit *et al*, 1994). Considering the above findings on the existence of three different hyaluronan synthases, it is likely that the expression of each hyaluronan synthase is regulated in a different manner, depending on the difference of growth regulatory factors or cytokines.

Langer and Vacanti (1993) described a new technology for solid organ transplants called *tissue engineering*, which involves the morphogenesis of new tissue using constructs formed from isolated cells cultured with growth regulatory factors and biocompatible scaffolds. Ueda *et al* (1995) fabricated cultured epithelium sheets for skin repair using cultured human oral mucosal epithelial (COME) cells and attained good clinical results. Therefore, we focused on the relationship among the growth regulatory factors, extracellular matrix, and epidermal and dermal cells, with the aim of tissue regeneration without scarring.

Most skin lesions heal rapidly and efficiently within a week or two; however, scars remain where the collagen matrix has been poorly reconstituted. Oral mucosa, on the other hand, rarely suffers from scarring in the process of

---

Abbreviations: COME cells, cultured human oral mucosal epithelial cells; EGF, epidermal growth factor; HA, hyaluronan; hHAS, human hyaluronan synthase; IL-1 $\beta$ , interleukin-1 $\beta$ ; ORF, open reading frame; PCR, polymerase chain reaction; RT-PCR, reverse transcriptase-polymerase

wound healing (Tsai *et al*, 1995) and appears to be different from skin in this regard. We have developed a method to fabricate cultured epithelium for skin repair using COME cells, which are a potential new source of cells for cultured epithelial grafts without scarring (Ueda *et al*, 1995). Therefore, comparison of the regulation of hyaluronan synthesis in oral mucosa with that in skin may yield important insights into the wound-healing processes characteristic of oral mucosa lesions. Histological analysis of the hyaluronan distribution in skin showed that this molecule is localized not only in the dermis but also in the epidermis (Tammi *et al*, 1984). The ability of keratinocytes to synthesize hyaluronan has been reported in both cell cultures (Brown and Parkinson, 1983) and organ cultures (Tammi *et al*, 1989; Agren *et al*, 1995). Skin grafts have been shown to promote wound closure by releasing a variety of cytokines (Krejci *et al*, 1991; Martin, 1997). Therefore, it is likely that the expression of three different hyaluronan synthases in the skin may be regulated by these factors. Actually, Sugiyama *et al* (1998) found that TGF- $\beta$  upregulates *HAS 1* and *HAS 2* expression independently in cultured human skin fibroblasts. Although *HAS 1*, *2*, and *3* mRNAs have been detected in various tissues by northern blot analyses (Spicer and McDonald, 1998), comparative studies on the distributions of *HAS 1*, *2*, and *3* expression as well as on the effect of cytokines on their expression between oral mucosa and skin have not yet been performed.

Real-time RT-PCR analysis enables one to detect quantitatively certain mRNAs in RNA samples, although careful attention must be paid to establishing suitable PCR conditions and primers (Gibson *et al*, 1996; Heid *et al*,

1996). In this study, we took advantage of this new method and also developed culture systems to assess the expression of the *HAS 1*, *HAS 2*, and *HAS 3* genes and hyaluronan synthesis in COME cells, oral mucosal fibroblasts, and skin dermal fibroblasts, and compared them before and after stimulation by IL-1 $\beta$  or EGF. The current results may help to clarify some of the mechanisms of the different responses in wound healing between oral mucosa and skin, and define potential targets for specific therapy directed at modulating hyaluronan synthesis in tissue engineering.

## Results

**Stimulation of expression of *HAS* genes by IL-1 $\beta$  or EGF in human mucosal COME cells** Using real-time RT-PCR analysis, we measured the absolute amounts of the mRNAs of the three different hyaluronan synthases, *HAS 1*, *HAS 2*, and *HAS 3*, in the COME cells. Comparisons of the expression among different samples by normalizing each of the absolute amounts enabled us to elucidate how the addition of IL-1 $\beta$  or EGF affected the expression of the *HAS 1*, *HAS 2*, and *HAS 3* genes. Treatment of COME cells with 0.1–100 ng per mL of IL-1 $\beta$  or EGF for 3 h resulted in a marked increase in both *HAS 1* and *HAS 2* mRNAs (Figs 1 and 2). Maximal levels of *HAS 1* and *HAS 2* expression were attained at 100 ng per mL IL-1 $\beta$  and 0.1 ng per mL EGF, respectively. Since EGF at this concentration (0.1 ng per mL) is used as one of the supplements for HuMedia-KG2 medium (commercially available), our finding indicates that this medium is suitable at least for hyaluronan synthesis by

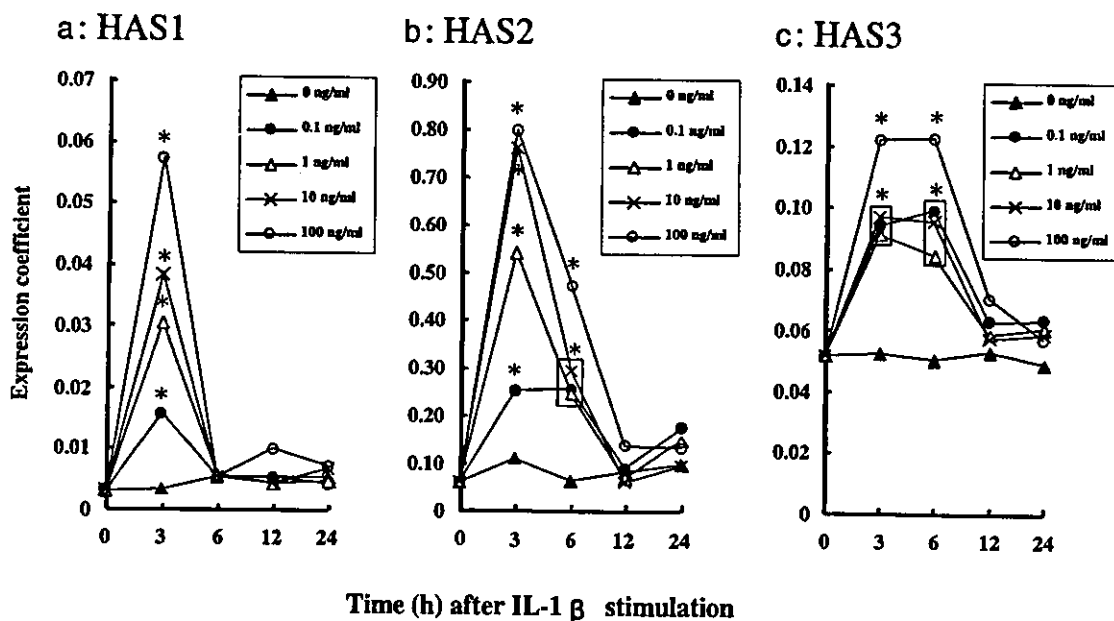


Figure 1

**Stimulation by IL-1 $\beta$  of *HAS 1* (a), *HAS 2* (b), and *HAS 3* (c) gene expression in COME cells.** COME cells were cultured in the presence of IL-1 $\beta$  at the indicated concentrations: 0 ng per mL ( $\blacktriangle$ ), 0.1 ng per mL ( $\bullet$ ), 1 ng per mL ( $\triangle$ ), 10 ng per mL ( $\times$ ), and 100 ng per mL ( $\circ$ ). After 3, 6, 12, and 24 h, cells were lysed and total RNA were extracted. Total RNA were also extracted from the cells just before adding IL-1 $\beta$  as a control (0 h). Equal amounts of total RNA (200 ng) were subjected to real-time RT-PCR analysis, and the absolute amounts of mRNA of *HAS 1*, *HAS 2*, *HAS 3*, and GAPDH in each sample were quantitated by comparison with their standard curves, as described in *Materials and Methods*. The expression coefficient for each mRNA (plotted on the ordinate) was calculated by dividing the absolute amount of each mRNA (*HAS 1*, *HAS 2*, and *HAS 3*) by the absolute amount of GAPDH mRNA in each sample so that quantitative comparisons of the expression of each *HAS* mRNA could be made among the different samples. Each point is the mean value obtained from five independent experiments in which the differences were less than 10%. \*Significantly different from the control value;  $p < 0.01$ . Boxed values are also significantly different ( $p < 0.01$ ) from the control.

Figure 2

**Stimulation by EGF of HAS1 (a), HAS2 (b), and HAS3 (c) gene expression in COME cells.** COME cells were cultured in the presence of EGF at the indicated concentrations: 0 ng per mL ( $\Delta$ ), 0.1 ng per mL ( $\bullet$ ), 1 ng per mL ( $\triangle$ ), 10 ng per mL ( $\times$ ), and 100 ng per mL ( $\circ$ ). After 3, 6, 12, and 24 h, cells were lysed and total RNA were extracted. Total RNA were also extracted from the cells just before the addition of EGF as a control (0 h). The ordinate represents the expression coefficient for each mRNA, which was calculated as described in Fig 1. Each point is the mean value obtained from five independent experiments in which the differences were less than 10%. \*Significantly different from the control value;  $p < 0.01$ . Boxed values are also significantly different ( $p < 0.01$ ) from the control.

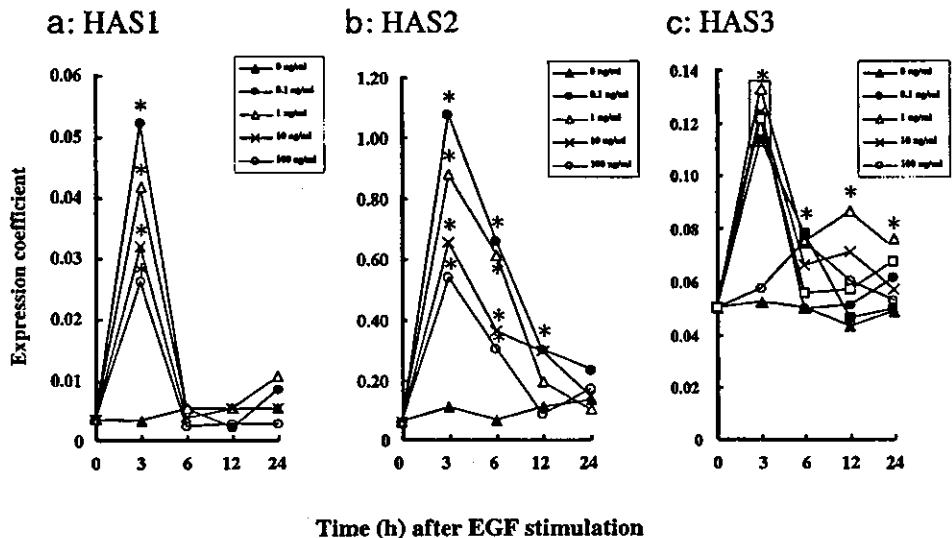
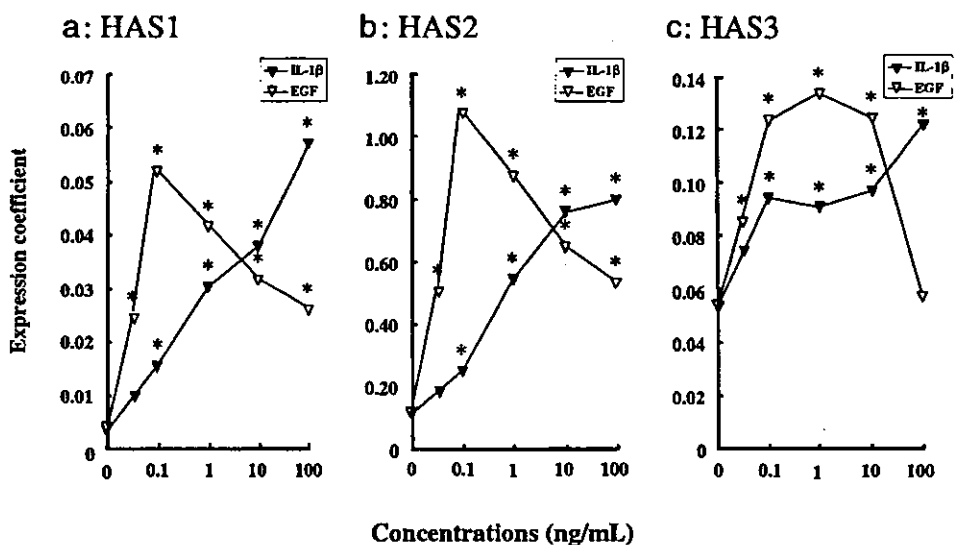


Figure 3

**Comparison of concentration-dependent changes of HAS1 (a), HAS2 (b), and HAS3 (c) gene expression between stimulation by IL-1 $\beta$  or EGF.** COME cells were cultured in the presence of the indicated concentrations of 0.1–100 ng per mL IL-1 $\beta$  ( $\nabla$ ) or EGF ( $\triangledown$ ). After 3 h, cells were lysed and total RNA were extracted. Total RNA were also extracted from the cells just before the treatment for the 0 h sample. Quantitation of each mRNA (HAS1, HAS2, and HAS3) was performed using equal amounts of total RNA (200 ng) by real-time RT-PCR as described in *Materials and Methods*. The ordinate represents the expression coefficient for each mRNA, which was calculated as described in Fig 1. Each point is the mean value obtained from five independent experiments in which the differences were less than 10%. \*Significantly different from the control value;  $p < 0.01$ .



COME cells. The amounts of HAS1 and HAS2 mRNAs were increased in a concentration-dependent manner by IL-1 $\beta$  at all concentrations tested, while those in EGF-treated COME cells were maximal at 0.1 ng per mL EGF and decreased to almost the basal level at the higher concentrations of EGF in order of HAS1 and HAS expression (Fig 3). A much smaller increase of HAS3 than of HAS1 and HAS2 expression was observed in the early phase of the stimulation (Figs 1 and 2). The concentration-dependent changes in HAS3 expression after IL-1 $\beta$  or EGF stimulation were similar to, but less marked than, those in HAS1 and HAS2 expression (Fig 3).

Comparisons of expression coefficients at 3 h, when the maximal stimulation was observed, suggested that the absolute amount of HAS2 mRNA was about 20-fold that of HAS1 mRNA, and about 8-fold that of HAS3 mRNA in COME cells (Figs 1–3). Therefore, the HAS2 mRNA appeared to be responsible for most of the hyaluronan synthase expression in the early phase of IL-1 $\beta$  or EGF stimulation. The proportion of HAS3 mRNA, however, appeared to become more significant in the late phase of the stimulation (Figs 1 and 2).

**Stimulation of HAS gene expression by IL-1 $\beta$  or EGF in cultured human oral mucosal and dermal fibroblasts** We examined the effects of IL-1 $\beta$  or EGF on the expression of HAS1, HAS2, and HAS3 mRNAs in cultured oral mucosal fibroblasts and dermal fibroblasts using the same method. Stimulation of these fibroblasts with 0.1–100 ng per mL IL-1 $\beta$  or EGF for 3 h resulted in a marked increase of HAS1 mRNA in cultured dermal fibroblasts, HAS2 mRNA in both dermal and cultured oral mucosal fibroblasts, and HAS3 mRNA in cultured oral mucosal fibroblasts. Maximal levels of HAS1 and HAS2 expression were attained at 1 ng per mL IL-1 $\beta$  in dermal fibroblasts, while those of HAS2 and HAS3 expression were attained at 1 ng per mL EGF in oral mucosal fibroblasts (Fig 4). Neither significant HAS1 gene expression in cultured oral mucosal fibroblasts nor HAS3 gene expression in dermal fibroblasts was detected at any concentration of EGF or IL-1 $\beta$  (Fig 4). Interestingly, lower expression of the HAS2 gene was observed in both types of fibroblasts after EGF stimulation compared with that after IL-1 $\beta$  stimulation, whereas the opposite was observed in COME cells after EGF and IL-1 $\beta$  stimulation

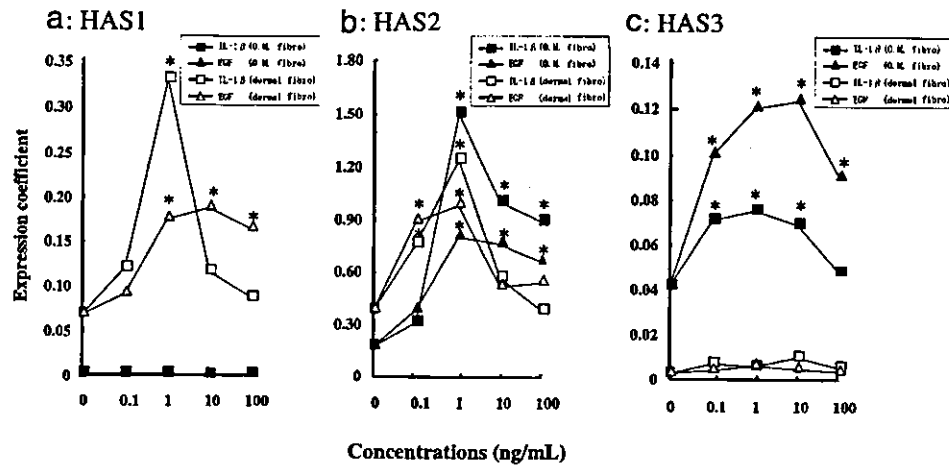


Figure 4

Comparison of concentration-dependent changes of HAS1 (a), HAS2 (b), and HAS3 (c) gene expression in oral mucosal and dermal fibroblasts between stimulation by IL-1 $\beta$  or EGF. Oral mucosal fibroblasts and dermal fibroblasts were cultured in the presence of the indicated concentrations of 0.1–100 ng per mL IL-1 $\beta$  (■ for oral mucosal fibroblasts, □ for dermal fibroblasts) or EGF (▲ for oral mucosal fibroblasts, △ for dermal fibroblasts) after 3 h, cells were lysed and total RNA were extracted. Total RNA were also extracted from the cells just before the treatment for the 0 h sample. Quantitation of each mRNA (HAS1, HAS2, and HAS3) was performed using equal amounts of total RNA (200 ng) by real-time RT-PCR as described in *Materials and Methods*. The ordinate represents the expression coefficient for each mRNA, which was calculated as described in Fig 1. Each point is the mean value obtained from five independent experiments in which the differences were less than 10%. \*Significantly different from the control value;  $p < 0.01$ .

(compare concentration-dependency in Fig 4 with that in Fig 3).

We then investigated the upregulation of the expression of HAS1, HAS2, and HAS3 mRNAs when oral mucosal and dermal fibroblasts were stimulated with 1 ng per mL IL-1 $\beta$  or EGF for different periods. Treatment of oral mucosal fibroblasts with IL-1 $\beta$  or EGF resulted in marked and moderate increases, respectively, in the amount of HAS2 mRNA, with maximal stimulations at 6 and 3 h, respectively (Figs 5 and 6). On the other hand, the amount of HAS3 mRNA in mucosal fibroblasts was increased time dependently for at least 24 h by IL-1 $\beta$  stimulation, but reached a plateau with a 2-fold increase at 3 h in response to EGF stimulation (Figs 5 and 6). When dermal fibroblasts were treated with IL-1 $\beta$  or EGF, the upregulation of expression of HAS1 and HAS2 mRNAs was observed as early as 3 h after stimulation with either agent. The amount of HAS1 mRNA, however, was further increased time

dependently up to 12 h, and then decreased to almost the basal level. The level of HAS2 mRNA was increased to a maximum at 6 h after IL-1 $\beta$  stimulation, decreased at 12 h, and again increased slightly thereafter. The maximal HAS2 expression level after IL-1 $\beta$  stimulation in dermal fibroblasts was 1.5 times higher than that after EGF stimulation (expression coefficient, 1.45 vs 0.93) (compare Fig 5 with Fig 6). The maximal stimulations by these cytokines of HAS1, HAS2, and HAS3 gene expression in both types of fibroblasts were mostly observed later than those in COME cells, as described above. The expression coefficients in Figs 5 and 6 suggest that in both types of cells, HAS2 mRNA was more abundant (about 5-fold) than the other HAS mRNAs.

These differences suggest that HAS1, HAS2, and HAS3 gene expression in oral mucosal and dermal fibroblasts is regulated by IL-1 $\beta$  and EGF in distinct manners that are cell-origin-specific and cytokine-specific.

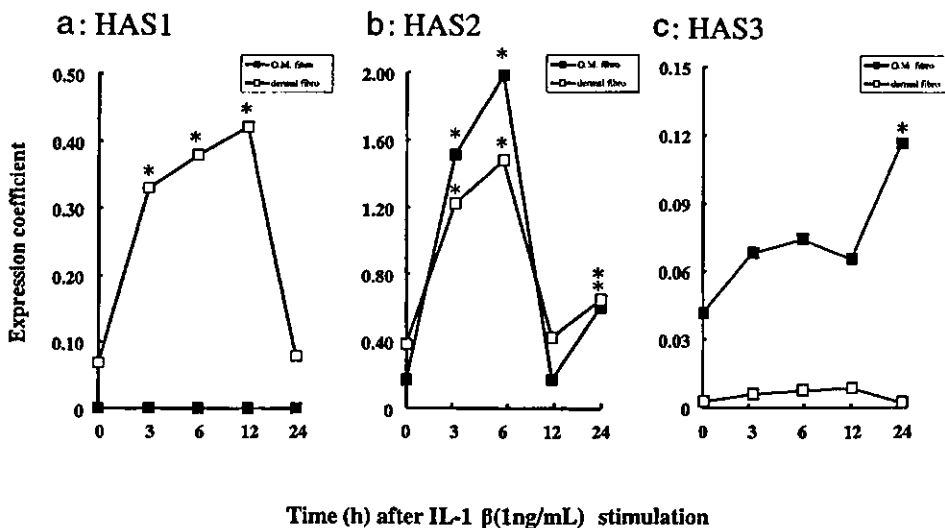
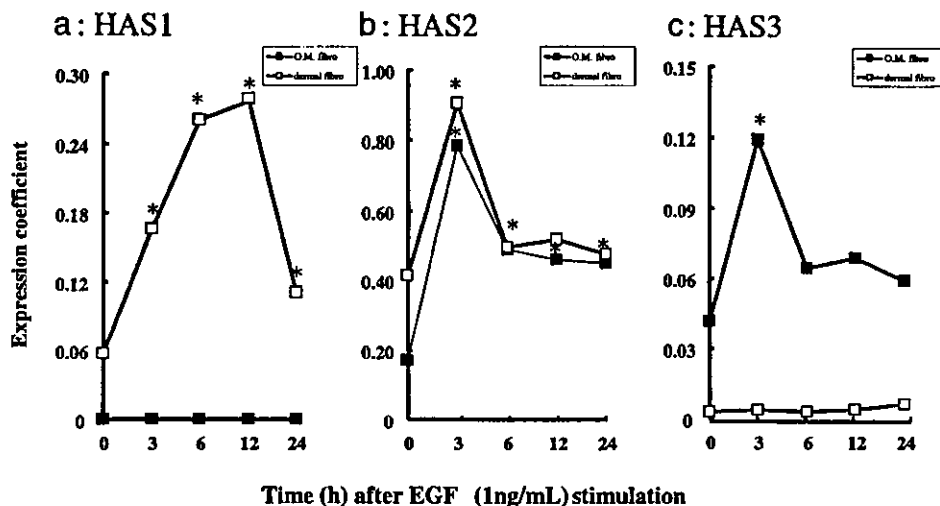


Figure 5

Comparison of stimulation by IL-1 $\beta$  of HAS1 (a), HAS2 (b), and HAS3 (c) gene expression between oral mucosal and dermal fibroblasts. Oral mucosal (■) and dermal (□) fibroblasts were cultured in the presence of 1 ng per mL IL-1 $\beta$ . After 3, 6, 12, and 24 h, cells were lysed and total RNA were extracted. For controls (0 h sample), total RNA were also extracted from the cells just before the addition of IL-1 $\beta$ . Quantitation of each mRNA (HAS1, HAS2, and HAS3) was performed using equal amounts of total RNA (200 ng) by real-time RT-PCR as described in *Materials and Methods*. The ordinate represents the expression coefficient for each mRNA, which was calculated as described in Fig 1. Each point is the mean value obtained from five independent experiments in which the differences were less than 10%. \*Significantly different from the control value;  $p < 0.01$ .



**Figure 6**  
**Comparison of stimulation by EGF of HAS1 (a), HAS2 (b), and HAS3 (c) gene expression between oral mucosal and dermal fibroblasts.** Oral mucosal (■) and dermal (□) fibroblasts were cultured in the presence of 1 ng per mL EGF. After 3, 6, 12, and 24 h, cells were lysed and total RNA were extracted. For controls (0 h sample), total RNA were also extracted from the cells just before the addition of EGF. Quantitation of each mRNA (HAS1, HAS2, and HAS3) was performed using equal amounts of total RNA (200 ng) by real-time RT-PCR as described in *Materials and Methods*. The ordinate represents the expression coefficient for each mRNA, which was calculated as described in Fig 1. Each point is the mean value obtained from five independent experiments in which the differences were less than 10%. \*Significantly different from the control value;  $p < 0.01$ .



**Time course of IL-1 $\beta$ - or EGF-induced hyaluronan synthesis in cultured human COME cells, oral mucosal, and dermal fibroblasts** To monitor the rate of hyaluronan synthesis at different times between 0 and 24 h after treatment with 1 ng per mL IL-1 $\beta$  or EGF, we measured the HA concentration in the culture medium at different times by a competitive ELISA-like assay, as shown in Fig 7. In COME cell cultures, IL-1 $\beta$  or EGF treatment induced an ~ 2–7-fold increase of newly synthesized hyaluronan during the stimulation, compared to the level at 3 h (Fig 7a). The amounts of HA in the cultures treated with either agent further increased time dependently up to 24 h. On the other hand, the amounts of HA in cultures of oral mucosal fibroblasts treated with IL-1 $\beta$  or EGF showed an ~ 23–47-fold increase, and that in cultures of dermal fibroblasts showed a 10–20-fold increase, compared to the levels at 3 and 6 h (Fig 7b, c). It is of note that neither oral mucosal fibroblasts nor dermal fibroblasts showed an IL-1 $\beta$ - or EGF-

induced increase in hyaluronan synthesis until 6 h and that higher levels of HA were generated in oral fibroblasts than in dermal fibroblasts after IL-1 $\beta$  stimulation (Fig 7b), whereas higher levels of HA were observed in dermal fibroblasts than in oral mucosal fibroblasts after EGF stimulation (Fig 7c). Overall, it was interesting to see that the increased expression levels of HAS after IL-1 $\beta$  or EGF stimulation resulted in increased rates of HA synthesis, although concentration dependency of the increase of HA synthesis by these agents remains to be determined.

**Discussion**

A major goal of wound-healing biology is to discover how skin can be induced to reconstruct damaged parts more perfectly (Martin, 1997). In this regard, we firstly noted the previous observation that oral mucosa rarely suffers from

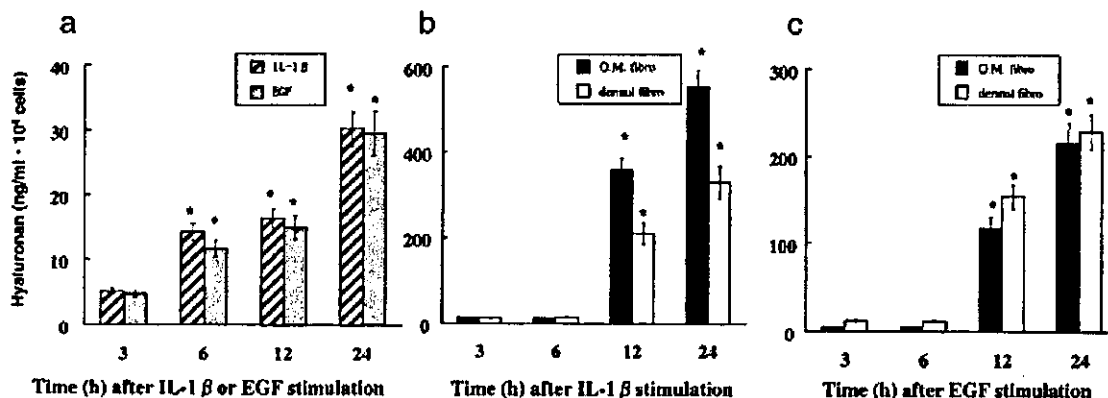


**Figure 7**  
**Time course of hyaluronan synthesis after the addition of IL-1 $\beta$  or EGF to COME cells (a), and after the stimulation of oral mucosal (■) and dermal fibroblasts (□) by IL-1 $\beta$  (b) or EGF (c).** HA concentrations of the conditioned media of 3, 6, 12, and 24 h cultures were measured by a competitive ELISA-like assay as described in *Materials and Methods*. Each value was calculated by subtracting the control value from the sample value. The control HA activities were about 14.3 (ng per mL 10<sup>4</sup> cells) in COME cells (a), 93.6 (ng per mL 10<sup>4</sup> cells) in oral mucosal fibroblasts, 115 (ng per mL 10<sup>4</sup> cells) in dermal fibroblasts, and these values varied only slightly at different times (3, 6, 12, and 24 h). (a) COME cells were cultured in the presence of 1 ng per mL IL-1 $\beta$  or EGF (b) Oral mucosal and dermal fibroblasts were cultured in the presence of 1 ng per mL IL-1 $\beta$ . (c) Oral mucosal and dermal fibroblasts were cultured in the presence of 1 ng per mL EGF. Each column represents the mean  $\pm$  SD of three separate experiments. \*Significantly different from the value at 3 h;  $p < 0.01$ .

scarring in the process of wound healing and appears to be different from skin (Tsai *et al*, 1995), and therefore focused on differences in physiological responses to wound healing between oral mucosa cells and skin cells in this study. Wound healing involves many dynamic cellular processes, such as cell proliferation, cell migration, cell-cell interaction, and inflammation (Martin, 1997). It has been found that hyaluronan is deeply involved in these dynamic cellular processes during wound healing and inflammation (Knudson *et al*, 1989; Turley, 1989; Weigel *et al*, 1997). It is also known that some cell growth factors and cytokines facilitate wound healing and re-epithelialization by stimulating keratinocyte proliferation and migration (Clark and Henson, 1988; Gailit *et al*, 1994; Hubner *et al*, 1996; Martin, 1997; Tammi and Tammi, 1998; Pienimaki *et al*, 2001). Therefore, in this study we examined the relationships between hyaluronan synthesis and cellular responses to two cell growth regulatory factors involved in wound healing of the skin, namely IL-1 $\beta$  and EGF.

The present results demonstrated that the expression of the three different HAS genes was increased in COME cells by IL-1 $\beta$  or EGF treatment, and there was a corresponding increase of hyaluronan synthesis in these cells after the treatments. Therefore, such treatments may induce changes in the extracellular environment via the increased synthesis and accumulation of hyaluronan. The present data also showed that the stimulations varied with different concentrations and times of treatment with the cytokines and that the stimulation patterns were highly dependent upon cell origins. This may be important for understanding the difference in wound healing between oral mucosal epithelium and epidermis.

Our present study did not focus on human keratinocytes, because they have already been studied in detail in a few studies, with the following results. Sugiyama *et al* (1998) showed that human keratinocytes expressed HAS1 mRNA and a trace of HAS2 mRNA, and that when the culture was stimulated with TGF- $\beta$ , HAS1 mRNA in keratinocytes was upregulated but HAS2 mRNA was not. A more recent study by Pienimaki *et al* (2001) showed that HAS2 mRNA was expressed in a rat keratinocyte cell line and EGF stimulation brought about an increase in HAS2 mRNA corresponding to about a 30-fold enhancement of hyaluronan production from the basal synthesis rate. They also showed that there was no increase in HAS1 or HAS3 in the cell line, but HAS2 mRNA increased 2-3-fold with less than 2 h following stimulation with EGF. Our present study on oral mucosal epithelium cells, however, demonstrated that in those cells the expression of HAS1 and HAS3 was upregulated after EGF stimulation, although these mRNAs were expressed at lower levels than HAS2 mRNA, and, in addition, HAS2 mRNA increased 2-11-fold depending on the concentration of the inducing agent (Fig 3). This finding may have depended on our use of the different cells or of the real-time RT-PCR method, which is more accurate than the methods used in earlier studies. Our finding also suggests that HAS1 and HAS3 might have distinctive effects on the wound healing of oral mucosal epithelia.

Sugiyama *et al* (1998) demonstrated that when human dermal fibroblasts were stimulated with TGF- $\beta$ , both HAS1 and HAS2 mRNAs were upregulated. Zhang *et al* (2000)

found by a quantitative study of HAS mRNA level that no HAS3 mRNA was detected in the RNA from human skin fibroblasts. We obtained similar results by quantitative real-time RT-PCR in our culture system of human dermal fibroblasts (Fig 4), although we used different cytokines. Our present study showed for the first time that HAS3 gene expression was detected in all of the mRNA samples obtained from human mucosal fibroblasts, but HAS1 gene expression was not detected. This unique HAS expression pattern of mucosal fibroblasts may be related to the unique feature of the lack of scarring in wound healing of oral mucosa epithelia.

It was interesting that the gradual increase in the amount of hyaluronan after the rapid and temporal increases in HAS mRNA expression after IL-1 $\beta$  or EGF treatment and the rates of hyaluronan synthesis differed, depending on the cell type and the stimulation agent (Fig 7). There have been several reports showing that the mRNA levels correlated with the levels of HAS proteins and with the production of hyaluronan (Jacobson *et al* (2000) for human mesothelial cells; Pienimaki *et al* (2001) for rat epidermal keratinocytes; Sayo *et al* (2002) for human keratinocytes). Pienimaki *et al* (2001) showed that the changes in HAS mRNA and hyaluronan synthesis levels showed a temporal correlation, suggesting tight transcriptional regulation of hyaluronan synthesis. In our study, however, in COME cells the hyaluronan synthetic rates increased gradually and time dependently with the maximal stimulation of the HAS mRNA expression at 3 h after IL-1 $\beta$  or EGF treatment, and the rate induced by IL-1 $\beta$  was higher than that induced by EGF. In both oral mucosal and dermal fibroblasts, the increased rates of hyaluronan synthesis were observed at later phases (12-24 h) than those of the mRNA expression. These differences suggest that the increased HAS enzyme proteins translated from the transiently increased amounts of the mRNAs resulting from the stimulation may have a long life span and produce hyaluronan continuously, especially in the cells stimulated by IL-1 $\beta$ . In addition, the turnover rates of the HAS mRNA may differ, depending on the cell type and way of stimulating the cells. In relation to the latter possibility, the gene structures, especially in the regulatory regions influencing the mRNA turnover, are different among the three HASs (Spicer and McDonald, 1998), and we previously characterized the promoter region of the mouse HAS1 gene (Yamada *et al*, 1998). Investigation of the respective promoter sequences and identification of potential enhancer sequences for the three HAS genes and the respective stability of those HAS mRNAs will be necessary for understanding the differences in the responses of the genes to stimulation by various factors.

Jacobson *et al* (2000) pointed out that the cytokine inducibility of the transcripts of the three HAS genes might be widespread, but differ depending on the cell type. Heldin *et al* (1989) also showed that cytokines and growth factors regulate the rates of hyaluronan synthesis differently, depending on the cell type. Since there were differences in the experimental systems and conditions, exact comparisons between studies cannot be made. There are several examples, however, in previous reports suggesting that the above possibility is true. For example, Kaback *et al* (1999) showed substantial upregulation of hyaluronan synthesis in

Table I. Sequences of oligonucleotide primers and real time RT-PCR probes

Primer or Probe	Sequence	Position
hHAS1 900F	TGTGTATCCTGCATCAGCGGT	900-920
hHAS1 1072R	CTGGAGGTGTACTTGGTAGCATAACC	1072-1047
hHAS1 probeF	TAACTCTTGCAGCAGTTTCTTGAGGCC	941-968
hHAS2 1475F	GTGTTATACATGTCGAGTTTACTTCC	1475-1496
hHAS2 1789R	GTCATATTGTTGTCCTTCTTCCGC	1789-1766
hHAS2 probeF	TGGAACGTTGCTCTATGCATGCTATTGG	1692-1719
hHAS3 83F	GGTACCATCAGAAGTTCCTAGGCAGC	83-108
hHAS3 411R	GAGGAGAATGTTCCAGATGCG	411-391
hHAS3 probeF	TGGCTACCGAACTAAGTATACCGCGCGCTC	158-188

mixture" was prepared according to the manufacturer's protocol to give final concentrations of  $1 \times$  avian myeloblastosis virus Tfl reaction buffer, 0.2 mM dNTPs, 1.5 mM MgSO<sub>4</sub>, 0.1 U per mL avian myeloblastosis virus reverse transcriptase, 0.1 U per  $\mu$ L Tfl DNA polymerase, 250 nM concentration of the primers, and 200 nM concentration of the corresponding probe, as described by Gibson *et al* (1996). Primers and probes for real-time PCR analysis of the hHAS1, hHAS2, and hHAS3 mRNAs were designed using the Oligo version 4.0 program (National Bioscience, Plymouth, Minnesota) according to Heid *et al* (1996). It has been shown that two or three transcripts that might be generated using alternative polyadenylation signals in the 3'-untranslated region exist for every HAS mRNA (Spicer and McDonald, 1998). In addition, there were differences in the 5'-terminal region sequence between the human HAS1 cDNAs cloned by us (Itano and Kimata, 1996b) and by Shyjan *et al* (1996). Therefore, this was taken into consideration when we designed the combinations of the primers. The sequences of all oligonucleotides used are shown in Table I. For the hHAS1 mRNA analysis, the primers hHAS1 900F and hHAS1 1072R were used and the probe was hHAS1TaqMan FP. For hHAS2 mRNA analysis, the primers hHAS2 1475F and hHAS2 1789R were used and the probe was hHAS2 TaqMan FP. For hHAS3 mRNA analysis, the primers hHAS3 83F and hHAS3 411R were used and the probe was hHAS3 TaqMan FP. The GAPDH primer and probe (TaqMan GAPDH detection reagents) were purchased from Perkin-Elmer and Applied Biosystems, Foster City, CA. RT-PCR reactions and the resulting relative increases in reporter fluorescent dye emissions were monitored in real time using a 7700 sequence detector (Perkin-Elmer). Signals were analyzed using the sequence detector 1.0 program (Perkin-Elmer). The conditions for PCR were as follows: an initial incubation at 50°C for 2 min, at 60°C for 30 min, and at 95°C for 5 min, followed by 50 cycles of incubation at 95°C for 20 s and 60°C for 1 min.

The absolute amount of each HAS mRNA in a given sample was obtained by comparison with the respective standard curves. Standard curves for each HAS mRNA were obtained using human heart t-RNA (Clontech, Palo Alto, California) with different concentrations (4000, 2000, 1000, 500, 250, 125, and 62.5 ng). Comparisons of the absolute amount of each mRNA for the three different HAS synthases among the different samples were made by using factors that were obtained by dividing the absolute amount of each mRNA by that of the GAPDH mRNA in each sample, and were designated as expression coefficients in this study.

**Determination of HA concentrations by competitive ELISA-like assay** Exponentially growing cells were cultured in fresh medium for 3, 6, 12, or 24 h, and the conditioned medium was recovered from each culture. The HA content of the conditioned medium was measured by a competitive ELISA-like assay as described

previously (Itano *et al*, 1999). Briefly, the conditioned medium was mixed with biotinylated HA binding protein (b-HABP) and incubated at 4°C for 20 h. The mixture was added to the HA-coated wells of 96-well plates, followed by incubation for 6 h at room temperature. Alkaline phosphatase-conjugated streptavidin was used as the secondary probe, and the enzymatic activity was measured by using *p*-nitrophenyl phosphate as the substrate. HA contents were calculated by using a standard curve.

**Statistical analysis** The Dunnett test was used for comparisons between control and experimental groups (Dunnett, 1964).

We are grateful to Drs Yukio Sumi, Hirokazu Mizuno, and Yuko Ito in the Department of Oral and Maxillofacial Surgery, to Yoshihisa Miyata in the Department of Dermatology, Nagoya University Graduate School of Medicine, to Dr Takao Kondo and Chiaki Inoue in the Department of Biology, Faculty of Science, Nagoya University, and to Manami Nagano at PE Applied Biosystems Field Application/Technical Support, Japan for help and technical advice, and to Drs. Masahiko Zako, Hidekazu Takagi, and Mamoru Yoshida for discussions. This work was supported in part by a Grant-in-Aid for Scientific Research on Priority Areas from the Ministry of Education, Culture, Sports, Science and Technology (MEXT); by a Grant-in-Aid for Young Scientists (B) from the Japan Society for the Promotion of Science; by a Grant-in-Aid for Science Research (B) from MEXT; by a Grant-in-Aid for research at the Matrix Glycoconjugate group, Research Center for Infectious Disease, Aichi Medical University, from MEXT; and by a special research fund from Seikagaku Corp.

DOI: 10.1111/j.0022-202X.2004.22332.x

Manuscript received July 23, 2003; revised September 30, 2003; accepted for publication November 4, 2003

Address correspondence to: Assistant Professor Yoichi Yamada, Center for Genetic and Regenerative Medicine, Nagoya University School of Medicine, 65 Tsuruma-cho, Showa-ku, Nagoya 466-8550, Japan. Email: yyamada@tsuru.med.nagoya-u.ac.jp

## References

- Agren UM, Tammi M, Tammi R: Hydrocortisone regulation of hyaluronan metabolism in human skin organ culture. *J Cell Physiol* 164:240-248, 1995
- Boyce ST, Ham RG: Calcium-regulated differentiation of normal human epidermal keratinocytes in chemically defined clonal culture and serum free serial culture. *J Invest Dermatol* 81:33-40, 1983
- Brown KW, Parkinson: Glycoproteins and glycosaminoglycans of cultured normal human epidermal keratinocytes. *J Cell Sci* 61:325-338, 1983

orbital fibroblasts when they were activated with IL-1 $\beta$ . Hyaluronan synthesis in human synovial lining cells is stimulated by TGF- $\beta$  and IL-1 $\beta$ , and to a lesser extent by TNF- $\alpha$ , and these cytokines have been suggested to be major factors leading to the development of joint swelling in inflammatory and degenerative joint diseases (Tammi and Tammi, 1998). In human keratinocytes, interferon- $\gamma$  markedly upregulates HAS3 mRNA, whereas transforming growth factor  $\beta$  downregulates HAS3 transcript levels (Sayo *et al*, 2002). We found that in COME cells stimulated by IL-1 $\beta$  or EGF, there was a smaller increase of HAS3 expression compared to HAS1 and HAS2 expression at an early phase of the stimulation (Figs 1 and 2). Human peritoneal mesothelial cells also show a pronounced increase in hyaluronan synthesis upon IL-1 $\beta$  stimulation, and the resultant increase in the hyaluronan level in the peritoneal cavity was suggested to be relevant to the inflammation in peritonitis (Yung *et al*, 1996). In the mesothelial cells, the IL-1 $\beta$  stimulation caused a continuous time-dependent increase in hyaluronan synthesis, which appeared to be different from our present results demonstrating rapid and temporary stimulation of the expression of all of the HAS genes by IL-1 $\beta$  (Figs 1, 3, and 5). The effect of EGF on the hyaluronan synthesis in human foreskin fibroblasts did not show a sharp dependency on the EGF concentration (Heldin *et al*, 1989), but we found that the effect on HAS mRNA expression in oral mucosal fibroblasts and dermal fibroblasts did (Fig 4). Taken together, these facts imply that it is likely that different regulatory mechanisms for the expression of each of the three HAS genes and the stability of their transcripts control hyaluronan synthesis in different cells, which might lead to important differences in the physiological responses between oral mucosa cells and skin cells.

The general tendency for EGF to inhibit terminal differentiation and the ability of EGF to increase the synthesis of hyaluronan, which we observed in the present experiments, may be in accord with the previous results on the treatment of keratinocytes with hydrocortisone (Agren *et al*, 1995) and retinoic acid (Tammi *et al*, 1989), further strengthening the concept that enhanced hyaluronan synthesis is associated with the delayed cornification of keratinocytes and subsequent epidermal thickening (Clark and Henson, 1988; Tammi and Tammi, 1998). Therefore, regulating hyaluronan synthesis by using the cytokines EGF or IL-1 $\beta$  might be useful for adjusting the levels of hyaluronan in skin cells to levels equal to those in oral mucosal cells, and might thereby promote wound healing without scarring in the skin if this is applied to tissue engineering technology using living cells, cytokines, and growth factors.

### Materials and Methods

**Cell culture and RNA isolation** Skin and oral mucosa (superfuous tissue obtained during surgery) were obtained from five patients treated in the Department of Oral Surgery and Plastic Surgery, Nagoya University Hospital. Donors gave informed consent. The cells were isolated by the method of Hata *et al* (1995). COME cells were routinely grown in HuMedia-KG2 medium (Kurabo, Osaka, Japan) (Boyce *et al*, 1983), supplemented with insulin (10  $\mu$ g per mL),

hydrocortisone (0.5  $\mu$ g per mL), 4% (v/v) bovine pituitary extract, and EGF (0.1 ng per mL) plus various antibiotics.

To study the effects of IL-1 $\beta$  and EGF, COME cells were expanded by culturing in HuMedia-KG2 medium with the above supplements for 5 d. The cells were thoroughly washed with the medium without the supplements, dissociated by treatment with trypsin, and inoculated into plastic tissue culture dishes (35 mm) containing fresh medium at a density of  $5.0 \times 10^5$  cells in the medium without EGF. At 48 h, the medium was exchanged and IL-1 $\beta$  or EGF (0.1–100 ng per mL) was added to the medium, and the cells were continuously cultured for the indicated times (0, 3, 6, 12, and 24 h). Total RNAs were extracted from the cells with an RNeasy Mini Kit (QIAGEN, GmbH, Hilden, Germany).

Human oral mucosal and dermal fibroblasts were grown in Dulbecco's modified Eagle's medium (DMEM) (Gibco Laboratories, Rockville, MD) containing 10% (v/v) fetal bovine serum and various antibiotics. In order to make the culture conditions identical to those used for studies on the stimulation of COME cells by IL-1 $\beta$  or EGF, the cells were grown for 14 d, dissociated with trypsin, and inoculated into plastic culture dishes (35 mm in diameter) at a density of  $5.0 \times 10^5$  cells with HuMedia-KG2 medium as described above. At 48 h, the medium was refreshed and IL-1 $\beta$  or EGF was added to the medium at 0.1–100 ng per mL. The cells were then cultured for 0, 3, 6, 12, and 24 h and total RNAs were extracted as described above.

**Preparation of absolute amounts of HAS1, HAS2, and HAS3 mRNAs** Samples containing known amounts of HAS1, HAS2, and HAS3 RNAs were prepared for absolute comparison by real-time RT-PCR analysis. HAS1 cDNA was prepared as described previously (Itano and Kimata, 1996b). HAS2 and HAS3 cDNAs were obtained by PCR with the following pairs of primers—dGTGTTATACATGTCGAGTTTACTTCC (position 1475–1496 of the human HAS2 ORF sequence) and dGTCATATTGTTGCCCTTCTTCCGC (position 1789–1766), and dGGTACCATCAGAAGTTCC-TAGGCAGC (position 83–108 of the human HAS3 ORF sequence) and dGAGGAGAATGTTCCAGATGCG (position 411–391), respectively—and subcloned into pBluescript II KS vector (Promega, Madison, Wisconsin). The PCR amplification was carried out by 35 cycles of incubation, with each cycle consisting of denaturation at 94°C for 20 s, annealing at 58°C for 30 s, and extension at 68°C for 8 min. The PCR products were checked by electrophoresis on a 2% (w/v) agarose gel. The cDNAs were confirmed by sequencing these products. The DNAs containing the respective HAS cDNAs downstream of the T7 promoter were constructed and used as templates to synthesize RNAs *in vitro* by incubation with T7 RNA polymerase (Boehringer, Mannheim, Germany) according to the manufacturer's protocol. The RNAs were purified with an RNeasy Mini Kit (QIAGEN). The concentration of each RNA sample was determined by measuring the absorption ( $A_{260}$ ) with a spectrophotometer.

**Real-time RT-PCR analysis** Real-time RT-PCR analysis was performed according to the reported method (Gibson *et al*, 1996; Heid *et al*, 1996). Briefly, within a gene-specific PCR oligonucleotide primer pair, an oligonucleotide probe labeled with a reporter fluorescent dye (FAM) at the 5'-end and a quencher fluorescent dye (TAMURA) at the 3'-end was designed. When the probe was intact, the reporter dye emission was quenched. During the extension phase of the PCR cycle, the nucleolytic activity of the DNA polymerase cleaved the hybridization probe and released the reporter dye from the probe. Fluorescence intensity produced during PCR amplifications was monitored by a sequence detector directly in the reaction tube ("real time"). A computer algorithm compared the amount of reporter dye emission with the quenching dye emission and calculated the threshold cycle number ( $C_T$ ) when signals reached ten times the standard deviation of the baseline, from which the levels of the mRNAs transcribed from the various genes tested were obtained (Gibson *et al*, 1996).

Total RNA samples (200 ng of each) were added to a 50  $\mu$ L RT-PCR reaction (PCR-Access, Promega). The "reaction master

- Brown GL, Curtsinger L, Brightwell JR, et al: Enhancement of epidermal regeneration by biosynthetic epidermal growth factor. *J Exp Med* 163:1319-1324, 1986
- Clark RAF, Henson PM: *The Molecular and Cellular Biology of Wound Repair*. New York: Plenum Press, 1988; p 3-33
- Dunnett CW: New tables for multiple comparisons with a control. *Biometrics* 20:482-491, 1964
- Gailit J, Welch MP, Clark RA: TGF-beta 1 stimulates expression of keratinocyte integrins during re-epithelialization of cutaneous wounds. *J Invest Dermatol* 103:221-227, 1994
- Gibson UEM, Heid CA, Williams A: Novel method for real time quantitative RT-PCR. *Genome Res* 6:995-1001, 1996
- Goliger JA, Paul DL: Wounding alters epidermal connexin expression and gap junction-mediated intercellular communication. *Mol Biol Cell* 6:1491-1501, 1995
- Hata K, Kagami H, Ueda M, Trii S, Matsuyama M: The characteristics of cultured mucosal cell sheet as a material for grafting: Comparison with cultured epidermal cell sheet. *Ann Plast Surg* 34:530-538, 1995
- Heid CA, Stevens J, Williams PM: Real time quantitative PCR. *Genome Res* 6:986-994, 1996
- Heldin P, Laurent TC, Heldin CH: Effect of growth factors on hyaluronan synthesis in cultured human fibroblasts. *Biochem J* 258:919-922, 1989
- Hubner G, Brauchle M, Smola H, et al: Differential regulation of pro-inflammatory cytokines during wound healing in normal and glucocorticoid-treated mice. *Cytokine* 8:548-556, 1996
- Itano N, Kimata K: Expression cloning and molecular characterization of HAS protein, a eukaryotic hyaluronan synthase. *J Biol Chem* 271:9875-9878, 1996a
- Itano N, Kimata K: Molecular cloning of human hyaluronan synthase. *Biochem Biophys Res Commun* 222:816-820, 1996b
- Itano N, Sawai T, Yamada Y, et al: Three isoforms of mammalian hyaluronan synthase have distinct enzymatic properties. *J Biol Chem* 274:25085-25092, 1999
- Jacobson A, Brinck J, Briskin MJ, Spicer AP, Heldin P: Expression of human hyaluronan synthases in response to external stimuli. *Biochem J* 348:29-35, 2000
- Kaback LA, Smith TJ: Expression of hyaluronan synthase messenger ribonucleic acids and their induction by interleukin-1 beta in human orbital fibroblasts: Potential insight into the molecular pathogenesis of thyroid-associated ophthalmopathy. *J Clin Endocrinol Metab* 84:4079-4084, 1999
- Knudson W, Biswas C, Li X-Q, Nemecek RE, Toole BP: The biology of hyaluronan. In: *Evered D, Whelan J (eds). Ciba Foundation Symposium, Vol. 143*. Chichester, UK: Wiley, 1989; p 150-169
- Krejci NC, Cuono CB, Langdon RC: *In vitro* reconstitution of skin: Fibroblasts facilitate keratinocyte growth and differentiation on acellular reticular dermis. *J Invest Dermatol* 97:843-848, 1991
- Langer R, Vacanti JP: Tissue engineering. *Science* 260:920-926, 1993
- Leibovich SJ, Ross R: The role of the macrophage in wound repair. A study with hydrocortisone and antimacrophage serum. *Am J Pathol* 78:71-100, 1975
- Martin P: Wound healing—Aiming for perfect skin regeneration. *Science* 276:75-81, 1997
- Pienimäki JP, Rilla K, Fulop C, et al: Epidermal growth factor activates hyaluronan synthesis 2 in epidermal keratinocytes and increases pericellular and intracellular hyaluronan. *J Biol Chem* 276:20428-20435, 2001
- Rosa F, Sargent TD, Rebbert ML, et al: Accumulation and decay of DG42 gene products follow a gradient pattern during *Xenopus* embryogenesis. *Dev Biol* 129:114-123, 1988
- Sayo T, Sugiyama Y, Takahashi Y, et al: Hyaluronan synthase 3 regulates hyaluronan synthesis in cultured human keratinocytes. *J Invest Dermatol* 118:43-48, 2002
- Shyjan A, Heldin P, Butcher E, Yoshino T, Briskin M: Functional cloning of the cDNA for a human hyaluronan synthase. *J Biol Chem* 271:23395-23399, 1996
- Spicer AP, Augustine ML, McDonald JA: Molecular cloning and characterization of putative mouse hyaluronan synthase. *J Biol Chem* 271:23400-23406, 1996
- Spicer AP, Olson JS, McDonald JA: Molecular cloning and characterization of a cDNA encoding the third putative mammalian hyaluronan synthase. *J Biol Chem* 272:8957-8961, 1997
- Spicer AP, McDonald JA: Characterization and molecular evolution of a vertebrate hyaluronan synthase gene family. *J Biol Chem* 273:1923-1932, 1998
- Sugiyama Y, Shimada A, Sayo T, Sakai S, Inoue SJ: Putative hyaluronan synthase mRNA are expressed in mouse skin and TGF-beta upregulates their expression in cultured human skin cells. *J Invest Dermatol* 110:116-121, 1998
- Tammi R, Ripellino JA, Margolis RU, Maibach HI, Tammi M: Hyaluronate accumulation in human epidermis treated with retinoic acid in skin. *J Invest Dermatol* 92:326-332, 1989
- Tammi R, Ripellino JA, Margolis RU, Tammi M: Localization of epidermal hyaluronic acid using the hyaluronate binding region of cartilage proteoglycan as a specific probe. *J Invest Dermatol* 90:412-414, 1988
- Tammi R, Tammi M: Glycoforum. Online (<http://www.glycoforum.gr.jp/>) 1-12, 1998
- Tsai CY, Hata K, Trii S, Matsuyama M, Ueda M: Contraction potency of hypertrophic scar-derived fibroblasts in a connective tissue model: *In vivo* analysis of wound contraction. *Ann Plast Surg* 35:638-646, 1995
- Turley EA: The biology of hyaluronan. In: *Evered D, Whelan J (eds). Ciba Foundation Symposium, Vol. 143*. Chichester, UK: Wiley, 1989; p 121-137
- Ueda M, Hata K, Horie K, Torii S: The potential of oral mucosal cells for cultured epithelium: A preliminary report. *Ann Plast Surg* 35:498-504, 1995
- Watanabe K, Yamaguchi Y: Molecular identification of a putative human hyaluronan synthase. *J Biol Chem* 271:22945-22948, 1996
- Weigel PH, Hascall VC, Tammi M: Hyaluronan synthases. *J Biol Chem* 272:13997-14000, 1997
- Yamada Y, Itano N, Zako M, et al: The gene structure and promoter sequence of mouse hyaluronan synthase 1 (mHAS1). *Biochem J* 330:1223-1227, 1998
- Yung S, Coles GA, Davies M: IL-1 beta, major stimulator of hyaluronan synthesis / *in vitro* of human peritoneal cells: Relevance to peritonitis in CAPD. *Kidney Int* 50:1337-1343, 1996
- Zhang W, Watson CE, Liu C, Williams KJ, Werth VP: Glucocorticoids induce a near-total suppression of hyaluronan synthase mRNA in dermal fibroblasts and in osteoblasts: A molecular mechanism contributing to organ atrophy. *Biochem J* 349:91-97, 2000

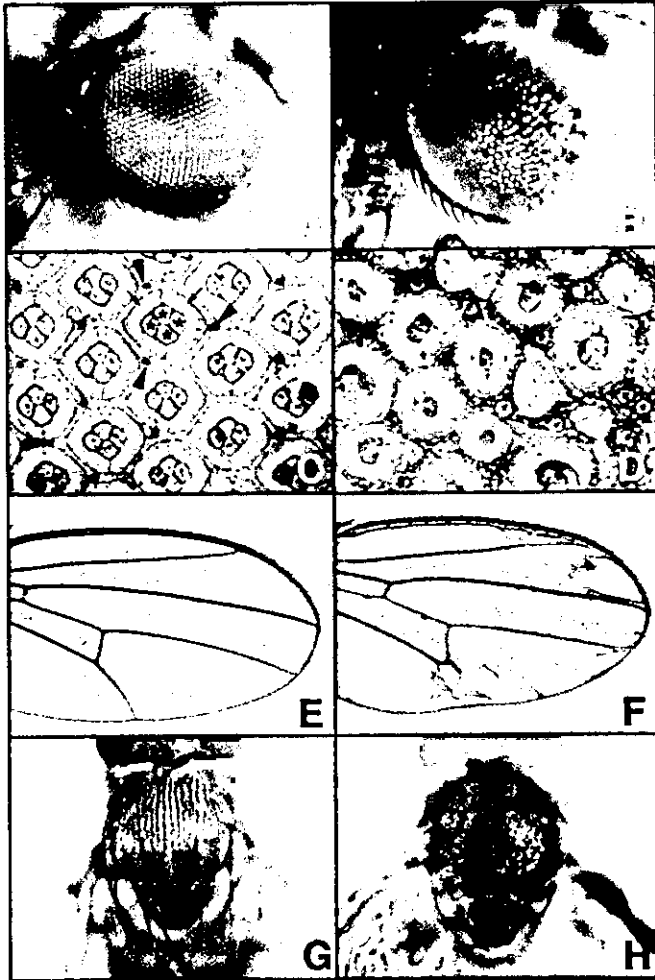


**FIG. 2. Expression of the *HAS2* gene disrupts normal morphogenesis in *Drosophila* tissues.** *A–D*, effect of *HAS2* expression on eye morphogenesis. Adult eyes (*A* and *B*) and pupal eyes stained with cobalt sulfide (*C* and *D*) are shown for wild-type animals (*A* and *C*) and animals with *HAS2*-expression by *CMR-GALA* (*B* and *D*). Cone cells (asterisks), pigment cells (arrows), and bristles (arrowheads) are shown. *E* and *F*, wild-type and *A9-GALA/UAS-HAS2-1* wings, respectively. *G* and *H*, effect of *HAS2* overexpression in the dorsal compartment of the wing disc. Wild-type and *UAS-HAS2-1/+;apterous-GALA/+* dorsal thoraxes are shown, respectively.

compromising DER signaling leads to reduced numbers of cone cells and pigment cells (33). On the other hand, an enlarged wing vein is a common phenotype observed upon reduction of Notch signaling (34, 35). In addition, the bristle phenotypes of *UAS-HAS2/+;apterous-GALA/+* flies resemble those of *warthog* (*wrt*) mutants (36). The *wrt* gene encodes a *Drosophila* homolog of Rab6, which regulates trafficking from the Golgi to the trans-Golgi network, and is required for proper secretion and cell-surface presentation of extracellular or transmembrane proteins. One of the signaling cascades affected by *wrt* mutations is the Notch pathway (37). It is therefore possible that some of *HAS2* overexpression phenotypes are a result of altered DER and/or Notch pathways. This observation suggests that *HAS2* expression interferes with cell-cell communications required for normal cell growth and differentiation during *Drosophila* tissue assembly.

***HAS2* Expression Does Not Affect the Levels of Other Glycosaminoglycans and Chitin**—Are the morphological defects of the *HAS2*-expressing animals caused by HA deposition? Alternatively, does *HAS2* expression affect the levels of other polysaccharides and therefore indirectly produce the phenotypes? In particular, because the biosynthesis of HA and heparan

sulfate, a different class of glycosaminoglycans, requires the common substrates UDP-GlcUA and UDP-GlcNAc, a possible explanation for these phenotypes could be interference with heparan sulfate synthesis; high levels of HAS protein may compete for the substrates with the endogenous heparan sulfate biosynthetic machinery. Indeed, a number of studies have demonstrated that heparan sulfate plays a critical role in *Drosophila* morphogenesis (for reviews, see Refs. 38–41). Similarly, synthesis of chondroitin sulfate and chitin, which need UDP-GlcUA and UDP-GlcNAc, respectively, may also be affected. To determine the effects of *HAS2* expression on the biosynthesis of chondroitin sulfate, heparan sulfate, and chitin, we measured the levels of these polysaccharides in the *HAS2*-expressing animals. As shown in Table I, we did not detect a significant change in the levels of these molecules upon expression of *HAS2*, although *UAS-HAS2-1/+;29BD-GALA/+* showed a moderately reduced level of heparan sulfate.

**Overexpression of UDP-glucose Dehydrogenase Enhances the Phenotype of *HAS2*-expressing Animals**—Several lines of information suggest that the moderate reduction of heparan sulfate in *UAS-HAS2-1/+;29BD-GALA/+* animals is unlikely to cause the morphological defects in the *HAS2*-expressing animals. First, reduced levels of heparan sulfate cannot explain the various phenotypes of *29BD-GALA/UAS-HAS2-2*, which showed a normal level of heparan sulfate (Table I). Second, we have several other transgenic strains that produce higher levels of HA and also show wild-type levels of heparan sulfate (data not shown); thus, HA production and heparan sulfate reduction do not seem to be directly correlated. To further examine whether the phenotypes associated with *HAS2* expression depend on the levels of HA or heparan sulfate, we performed a sensitive genetic assay in which the cellular levels of UDP-GlcUA were manipulated. If the *HAS2* overexpression phenotypes are caused by HA accumulation on the cell surface, these phenotypes should be enhanced by increasing the UDP-GlcUA level and should be suppressed by its reduction. The reverse will happen if these defects are consequences of loss of substrates and defective heparan sulfate-dependent signaling. Based on these criteria, we genetically manipulated the dosage of *sgl*, which encodes a UDP-glucose dehydrogenase, an essential enzyme for UDP-GlcUA biosynthesis (25, 42–45), and examined its effect on the rough eye phenotype of *GMR-GALA/+;UAS-HAS2/+* animals. As depicted in Fig. 3B, we did not detect a significant change in the phenotype by deleting one copy of *sgl*. On the other hand, overexpression of *sgl* by the transgene under the control of the ubiquitin promoter (*ubi-sgl*) (25) dramatically enhanced the eye defects, resulting in gross defects in eye formation with necrosis (Fig. 3D). This observation indicates that HA accumulation (but not disrupted heparan sulfate synthesis) is responsible for the morphological abnormalities in the *HAS2*-expressing animals.

**HA-synthesizing Wings Accumulate High Levels of Water**—The ability of HA to hold a large amount of water is an important biophysical property as a structural constituent of the extracellular matrix. We noticed that *HAS2* overexpression by the *UAS-HAS2-2* transgene under the control of *29BD-GALA* at 20 °C induced the characteristic wing phenotypes (Fig. 4, *B* and *B'*). These wings were thick and partly wrinkled, and the dorsal and ventral epithelial sheets were detached from each other. In addition, they were opaque compared with wild-type wings, which were transparent. Overall, the wings appeared to be swollen with fluid in their interior. Wings from *engrailed-GALA/+;UAS-HAS2-2/+* adults also exhibited a similar phenotype only in the posterior compartment (data not shown), confirming that this phenotype is associated with HA accumulation. To determine whether these wings show in-

TABLE II  
Phenotypes produced by expression of the *HAS2* gene in *Drosophila*

The phenotypes induced by *HAS2* expression by two independent transgenic strains (*UAS-HAS2-1* and *UAS-HAS2-2*) with each *GAL4* driver are shown. Expression of *UAS-HAS2-1*, which produces higher levels of HA, resulted in much more severe phenotypes compared with that of *UAS-HAS2-2*. Corresponding figures are shown in parentheses.

GAL4 lines	Expression	<i>UAS-HAS2-1</i>	<i>UAS-HAS2-2</i>
Actin 5C <i>29BD</i>	Ubiquitous Ubiquitous	Lethality (first instar larval stage) Lethality (pupal stage)	Lethality (pupal stage) Disordered wing veins, wet wing, eclosion defect (Fig. 4)
<i>GMR</i> <i>A9</i>	Eye disc Wing and halter discs	Severe rough eye Thickened and ectopic veins, extra notal bristles (Fig. 2F)	Mild rough eye (Fig. 3A) Disordered veins
<i>apterous</i>	Dorsal compartment of wing disc	Semilethality, eclosion defect, folded wing, abnormal shape and patterns of notal bristles (Fig. 2H)	Disordered veins
<i>engrailed</i>	Posterior compartment	Eclosion defect, folded wing	Disordered veins, wet wing

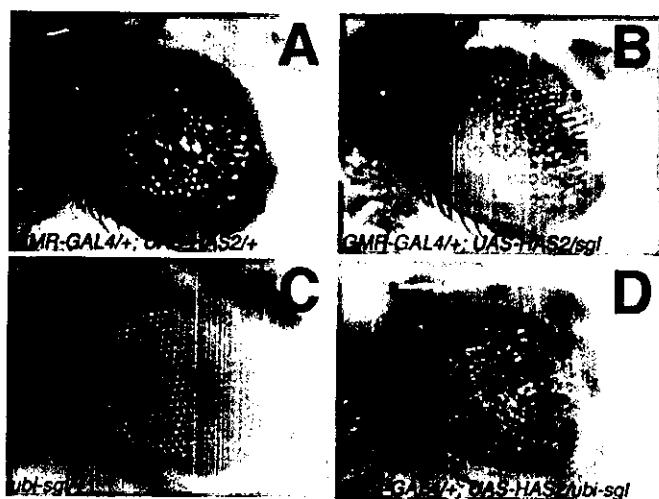


FIG. 3. Overexpression of *sgl* enhances the eye phenotype of *HAS2*-expressing animals. Adult eyes are shown for *GMR-GAL4/+; UAS-HAS2-2/+* (A), *GMR-GAL4/+; UAS-HAS2-2/sgl* (B), *ubi-sgl/+* (C), and *GMR-GAL4/+; UAS-HAS2-2/ubi-sgl* (D). Deleting one copy of the *sgl* gene did not affect the eye phenotype of *HAS2*-expressing animals. On the other hand, this phenotype was drastically enhanced by ubiquitous overexpression of *sgl*.

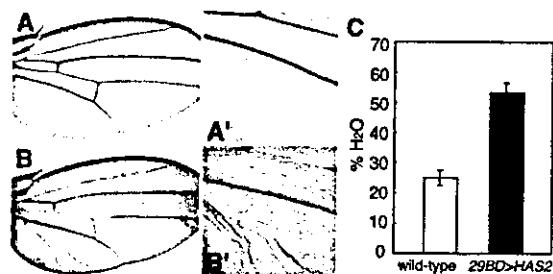


FIG. 4. *Drosophila* wings synthesizing HA show high water content. Wings are shown for wild-type (A and A') and *29BD-GAL4/UAS-HAS2-2* (B and B') animals. A' and B' are high magnification views of A and B, respectively. In C, the water content of adult wings was determined by the coulometric Karl-Fischer method (31, 32). Each error bar represents the S.E. of four and six measurements of wild-type and *29BD-GAL4/UAS-HAS2-2* wings, respectively. The difference among them is significant at the 1% level as determined by Mann-Whitney's *U* test ( $p = 0.0089$ ).

creased water content, we collected wild-type and *29BD-GAL4/UAS-HAS2-2* wings and measured H<sub>2</sub>O in these tissues by the Karl-Fischer titration, a well established method for determining water (31, 32). Indeed, the water content of wings that produced HA was considerably high, reaching twice as much as that of the wild-type wings (Fig. 4C). We therefore call this phenotype "wet wing" in Table II. Thus, HA synthesized in

*Drosophila* wing cells is capable of holding a high level of water and is likely to be functionally relevant to that synthesized in mammalian cells.

#### DISCUSSION

Insects produce cuticle, the chitin-based exoskeleton that prevents desiccation of body moisture. This structure enables these species to attain light body weight and to accommodate a large variety of living space. On the other hand, higher vertebrate animals employ HA, which ensures water inside the body. Thus, the life styles of animals are not unrelated to the polysaccharides they produce, and diversion of HA- and chitin-producing organisms could be one of the key steps in animal evolution. Recent studies suggest that the HAS and chitin synthase genes have evolved from a common origin. Here, we have provided evidence that HA can be produced by introducing a single HAS gene into a chitin-synthesizing multicellular organism, the *Drosophila* fruit fly, which normally does not synthesize HA. The HAS2 enzyme was active in such a heterologous system and efficiently synthesized a high level of HA without exogenously supplied substrates or primers. The observation that HA products were deposited on the cell surface implies that HAS acts in *Drosophila* cells as it functions in mammalian cells: it polymerizes HA chains at the inner face of the plasma membrane and coordinately secretes HA out of the cell. This result is significant because it is currently unclear whether proper elongation and secretion of HA require other proteinaceous and non-proteinaceous components in addition to HAS. Our finding of efficient HA production and secretion in insect cells strongly supports that such additional factors are not essential for normal HA biosynthesis. However, we cannot exclude the possibility that HAS2 accomplishes HA synthesis by utilizing the chitin biosynthetic machinery in *Drosophila* cells. Additional studies on the biosynthetic machineries of HA and chitin will clarify this point. Thus, the *Drosophila* system will provide new insights into unsolved problems regarding HA biosynthesis.

The *HAS2*-overexpressing flies showed a variety of phenotypes in many tissues. The biochemical and genetic experiments showed that these phenotypes are caused by accumulation of HA in tissues, but not by lack of chondroitin sulfate, heparan sulfate, or chitin. How did HA synthesis induce such phenotypes? In the HA network in a physiological solution, diffusion rates of macromolecules such as proteins are expected to be slow, and the concentration of these molecules will be lower in the network compared with an HA-free environment. This would explain the observed morphological defects. The abnormalities caused by *HAS2* expression are reminiscent of phenotypes caused by disruption of intercellular signaling mediated by extracellular or cell-surface signaling molecules, the movement of which will be restricted in the HA network. For

example, disruption of diffusion of Spitz, a secreted ligand of DER, may result in a similar phenotype compared with that of *HAS2* overexpression (33). Another explanation for these phenotypes is that a particular signaling pathway is ectopically activated by HA in *Drosophila* cells. Recent mounting evidence suggests that HA triggers multiple signaling pathways (for review, see Ref. 46), and counterparts of many of these signaling components exist in flies. It is therefore possible that synthesized HA abnormally activates such cascade(s) and interferes with normal morphogenesis. Finally, some of the phenotypes appear to be a direct result of the biophysical property of HA itself. Interestingly, quantification of the water content of *Drosophila* tissues with or without HA revealed that HA produced in *Drosophila* cells shows hydrodynamic properties relevant to those of mammalian HA; HA created a new extracellular matrix, which was swollen with water.

The eye phenotype of *HAS2*-overexpressing animals was strongly enhanced by coexpression of the *sgl* gene, which encodes a UDP-glucose dehydrogenase. It is worth noting that a substantial effect of increasing the level of UDP-glucose dehydrogenase on the phenotype is consistent with the prediction that substrate availability is a limiting factor in HA biosynthesis (44). Although we have not tested the effects of alterations in UDP-GlcNAc levels on HA deposition, it is possible that the cytosolic concentration of UDP-GlcNAc might be high in insect cells that synthesize chitin, a GlcNAc polymer, at the inner face of the plasma membrane and is therefore less critical than the UDP-GlcUA level.

The consequences of lack or elevation of HA synthesis have become the recent focus of intense research interest. Camenisch *et al.* (18) showed that *HAS2*-deficient mice exhibit serious cardiovascular defects. An explant system using *HAS2*<sup>-/-</sup> tissue was used to demonstrate that HA is essential for a cell migration event required for cardiac cushion morphogenesis. Interestingly, ectopic deposition of HA also affects cell migration and adhesion (20). Stable HAS transfectants in non-transformed rat 3Y1 cells show reduced contact inhibition of cell growth and migration. HA overproduction in these cells also alters the microfilament organization and N-cadherin distribution at the intercellular boundaries. These phenotypes are suppressed by treatment with inhibitors of phosphatidylinositol 3-kinase, suggesting that phosphatidylinositol 3-kinase signaling mediates the HA-dependent aberration of contact inhibition. This line of studies will further improve our understanding of HA functions in cell behavior and signaling. Our present study illustrates the possibility that a model system using the genetically tractable organism *Drosophila* could be a strategy to study *in vivo* roles as well as evolution of the biosynthetic machinery of polysaccharides. Furthermore, given that insect cells are cheap and easy to handle, the fact that these cells can produce HA without any exogenous supply of donor substrates will be useful information for medical and pharmaceutical applications of HA.

**Acknowledgments**—We thank J. A. McDonald (Mayo Clinic, Scottsdale, AZ) for the kind gift of the mouse *HAS2* cDNA. We are grateful to M. B. O'Connor and the Bloomington Stock Center for fly stocks. We also thank F. Kato, M. Suzuki, and N. Sugiura (Seikagaku Co.) for

assistance in quantification of the water content of *Drosophila* adult wings by the Karl-Fischer method.

## REFERENCES

- Toole, B. P. (1990) *Curr. Opin. Cell Biol.* **2**, 839–844
- Yoshida, M., Itano, N., Yamada, Y., and Kimata, K. (2000) *J. Biol. Chem.* **275**, 497–506
- Isacke, C. M., and Yarwood, H. (2002) *Int. J. Biochem. Cell Biol.* **34**, 718–721
- Turley, E. A. (1992) *Cancer Metastasis Rev.* **11**, 21–30
- Turley, E. A., Noble, P. W., and Bourguignon, L. Y. (2002) *J. Biol. Chem.* **277**, 4589–4592
- Bono, P., Rubin, K., Higgins, J. M., and Hynes, R. O. (2001) *Mol. Biol. Cell* **12**, 891–900
- Itano, N., and Kimata, K. (1996) *J. Biol. Chem.* **271**, 9875–9878
- Shyjan, A. M., Heldin, P., Butcher, E. C., Yoshino, T., and Briskin, M. J. (1996) *J. Biol. Chem.* **271**, 23395–23399
- Itano, N., and Kimata, K. (1996) *Biochem. Biophys. Res. Commun.* **222**, 816–820
- Spicer, A. P., Augustine, M. L., and McDonald, J. A. (1996) *J. Biol. Chem.* **271**, 23400–23406
- Watanabe, K., and Yamaguchi, Y. (1996) *J. Biol. Chem.* **271**, 22945–22948
- Fulop, C., Salustri, A., and Hascall, V. C. (1997) *Arch. Biochem. Biophys.* **337**, 261–266
- Spicer, A. P., Olson, J. S., and McDonald, J. A. (1997) *J. Biol. Chem.* **272**, 8957–8961
- Spicer, A. P., Seldin, M. F., Olsen, A. S., Brown, N., Wells, D. E., Doggett, N. A., Itano, N., Kimata, K., Inazawa, J., and McDonald, J. A. (1997) *Genomics* **41**, 493–497
- Spicer, A. P., and McDonald, J. A. (1998) *J. Biol. Chem.* **273**, 1923–1932
- Itano, N., Sawai, T., Miyaishi, O., and Kimata, K. (1999) *Cancer Res.* **59**, 2499–2504
- Itano, N., Sawai, T., Yoshida, M., Lenas, P., Yamada, Y., Imagawa, M., Shinomura, T., Hamaguchi, M., Yoshida, Y., Ohnuki, Y., Miyauchi, S., Spicer, A. P., McDonald, J. A., and Kimata, K. (1999) *J. Biol. Chem.* **274**, 25085–25092
- Camenisch, T. D., Spicer, A. P., Brehm-Gibson, T., Biesterfeldt, J., Augustine, M. L., Calabro, A., Jr., Kubalak, S., Klewer, S. E., and McDonald, J. A. (2000) *J. Clin. Invest.* **106**, 349–360
- Camenisch, T. D., Schroeder, J. A., Bradley, J., Klewer, S. E., and McDonald, J. A. (2002) *Nat. Med.* **8**, 850–855
- Itano, N., Atsumi, F., Sawai, T., Yamada, Y., Miyaishi, O., Senga, T., Hamaguchi, M., and Kimata, K. (2002) *Proc. Natl. Acad. Sci. U. S. A.* **99**, 3609–3614
- DeAngelis, P. L., and Achyuthan, A. M. (1996) *J. Biol. Chem.* **271**, 23657–23660
- Rubin, G. M., and Spradling, A. C. (1982) *Science* **218**, 348–353
- Brand, A. H., and Perrimon, N. (1993) *Development* **118**, 401–415
- Toba, G., Ohsako, T., Miyata, N., Ohtsuka, T., Seong, K. H., and Aigaki, T. (1999) *Genetics* **151**, 725–737
- Haerry, T. E., Heslip, T. R., Marsh, J. L., and O'Connor, M. B. (1997) *Development* **124**, 3055–3064
- Toyoda, H., Kinoshita-Toyoda, A., and Selleck, S. B. (2000) *J. Biol. Chem.* **275**, 2269–2275
- Reissig, J. L., Storminger, J. L., and Leloir, L. F. (1955) *J. Biol. Chem.* **217**, 959–966
- Lee, H. G., and Cowman, M. K. (1994) *Anal. Biochem.* **219**, 278–287
- Zhang, M., Haga, A., Sekiguchi, H., and Hirano, S. (2000) *Int. J. Biol. Macromol.* **27**, 99–105
- Wolff, T., and Ready, D. F. (1991) *Development* **113**, 825–839
- Fischer, K. A. (1935) *Angew. Chem. Int. Ed. Engl.* **48**, 394–396
- Thiex, N. J., and Van Erem, T. (2002) *J. Assoc. Off. Anal. Chem. Int.* **85**, 318–327
- Freeman, M. (1996) *Cell* **87**, 651–660
- de Celis, J. F., Bray, S., and Garcia-Bellido, A. (1997) *Development* **124**, 1919–1928
- Huppert, S. S., Jacobsen, T. L., and Muskavitch, M. A. (1997) *Development* **124**, 3283–3291
- Purcell, K., and Artavanis-Tsakonas, S. (1999) *J. Cell Biol.* **146**, 731–740
- Verheyen, E. M., Purcell, K. J., Fortini, M. E., and Artavanis-Tsakonas, S. (1996) *Genetics* **144**, 1127–1141
- Bernfield, M., Gotte, M., Park, P. W., Reizes, O., Fitzgerald, M. L., Liucceum, J., and Zako, M. (1999) *Annu. Rev. Biochem.* **68**, 729–777
- Lander, A. D., and Selleck, S. B. (2000) *J. Cell Biol.* **148**, 227–232
- Selleck, S. B. (2000) *Trends Genet.* **16**, 206–212
- Perrimon, N., and Bernfield, M. (2000) *Nature* **404**, 725–728
- Binari, R. C., Staveley, B. E., Johnson, W. A., Codavarti, R., Sasisekharan, R., and Manoukian, A. S. (1997) *Development* **124**, 2623–2632
- Hacker, U., Lin, X., and Perrimon, N. (1997) *Development* **124**, 3565–3573
- Spicer, A. P., Kaback, L. A., Smith, T. J., and Seldin, M. F. (1998) *J. Biol. Chem.* **273**, 25117–25124
- Walsh, E. C., and Staimier, D. Y. (2001) *Science* **293**, 1670–1673
- Lee, J. Y., and Spicer, A. P. (2000) *Curr. Opin. Cell Biol.* **12**, 581–586



## Characterization of Growth Factor-binding Structures in Heparin/Heparan Sulfate Using an Octasaccharide Library\*

Received for publication, December 10, 2003

Published, JBC Papers in Press, January 5, 2004, DOI 10.1074/jbc.M313523200

Satoko Ashikari-Hada<sup>‡§</sup>, Hiroko Habuchi<sup>‡</sup>, Yutaka Kariya<sup>§</sup>, Nobuyuki Itoh<sup>||</sup>,  
A. Hari Reddi<sup>||</sup>, and Koji Kimata<sup>‡\*\*</sup>

From the <sup>‡</sup>Institute for Molecular Science of Medicine, Aichi Medical University, Nagakute, Aichi 480-1195, <sup>§</sup>Central Research Laboratories, Seikagaku Corp., Tateno, Higashiyamato-shi, Tokyo 207-0021, <sup>||</sup>Department of Genetic Biochemistry, Kyoto University Graduate School of Pharmaceutical Sciences, Yoshida-Shimoadachi, Sakyo, Kyoto 606-8501, Japan, and <sup>||</sup>Center for Tissue Regeneration and Repair, University of California School of Medicine, Davis, California 95817

Heparan sulfate (HS) chains interact with various growth and differentiation factors and morphogens, and the most interactions occur on the specific regions of the chains with certain monosaccharide sequences and sulfation patterns. Here we generated a library of octasaccharides by semienzymatic methods by using recombinant HS 2-O-sulfotransferase and HS 6-O-sulfotransferase, and we have made a systematic investigation of the specific binding structures for various heparin-binding growth factors. An octasaccharide (Octa-I,  $\Delta$ HexA-GlcNSO<sub>3</sub>-(HexA-GlcNSO<sub>3</sub>)<sub>3</sub>) was prepared by partial heparitinase digestion from completely desulfated *N*-resulfated heparin. 2-O- and 6-O-sulfated Octa-I were prepared by enzymatically transferring one to three 2-O-sulfate groups and one to three 6-O-sulfate groups per molecule, respectively, to Octa-I. Another octasaccharide containing 3 units of HexA(2SO<sub>4</sub>)-GlcNSO<sub>3</sub>(6SO<sub>4</sub>) was prepared also from heparin. This octasaccharide library was subjected to affinity chromatography for interactions with fibroblast growth factor (FGF)-2, -4, -7, -8, -10, and -18, hepatocyte growth factor, bone morphogenetic protein 6, and vascular endothelial growth factor, respectively. Based upon differences in the affinity to those octasaccharides, the growth factors could be classified roughly into five groups: group 1 needed 2-O-sulfate but not 6-O-sulfate (FGF-2); group 2 needed 6-O-sulfate but not 2-O-sulfate (FGF-10); group 3 had the affinity to both 2-O-sulfate and 6-O-sulfate but preferred 2-O-sulfate (FGF-18, hepatocyte growth factor); group 4 required both 2-O-sulfate and 6-O-sulfate (FGF-4, FGF-7); and group 5 hardly bound to any octasaccharides (FGF-8, bone morphogenetic protein 6, and vascular endothelial growth factor). The approach using the oligosaccharide library may be useful to define specific structures required for binding to various heparin-binding proteins. Octasaccharides with the high affinity to FGF-2 and FGF-10 had the activity to release them, respectively, from their complexes with HS. Thus, the library may provide new reagents to specifically regulate bindings of the growth factors to HS.

Heparan sulfate (HS)<sup>1</sup> exists ubiquitously as a component of proteoglycans on cell surfaces and in extracellular matrix and basement membranes and has divergent structures and functions (1–3). HS chains are known to interact with a variety of proteins such as heparin-binding growth and differentiation factors (HBGFs), morphogens, extracellular matrix components, protease inhibitors, protease, lipoprotein lipase, and various pathogens (4–8). These interactions have been shown to play a pivotal role in various patho-physiological phenomena as well as in tissue morphogenesis, as uncovered by recent genetic studies (9–12). In some of these phenomena, the interactions of HS with certain proteins have been shown in regions of the HS with specific monosaccharide sequences and sulfation patterns. Such functional domains are thought to be generated after the sequential modification steps during the biosynthesis of HS. In these modification steps, HS *N*-deacetylase/*N*-sulfotransferases (13–16), C5 epimerase (17), HS 2-O-sulfotransferase (HS2ST) (18), HS 6-O-sulfotransferases (HS6ST) (19, 20), and HS 3-O-sulfotransferase (21, 22) are involved. The expression patterns of the individual modification enzymes have been shown to differ from tissue to tissue, and as a result different functional structures of HS may be generated in the different tissues. Such structural diversity introduced to HS may result in the different response of each tissue to various heparin-binding proteins.

So far, the sequences in HS that interact with FGF-1 or FGF-2 have been studied by biochemical and x-ray crystallographic analysis. It became apparent that the FGF-1-binding region was distinct from the minimal FGF-2-binding region (23–27). In addition to the studies on FGF-1 and FGF-2, the HS sequences that mediate binding and/or activation of some HBGFs have been reported in the systems including FGF-4 (23, 24), FGF-8b (28), hepatocyte growth factor (HGF) (29–31), and platelet-derived growth factor (32). These studies on the binding structures in HS appear to support the idea that each heparin-binding growth factor may recognize the respective

\* This work was supported in part by Grant-in-aid for Scientific Research on Priority Areas from the Ministry of Education, Culture, Sports, Science and Technology of Japan 14082206, by a preparatory grant for research at the Matrix Glycoconjugate Group, Research Center for Infectious Disease, Aichi Medical University, and by a special research fund from Seikagaku Corp. The costs of publication of this article were defrayed in part by the payment of page charges. This article must therefore be hereby marked "advertisement" in accordance with 18 U.S.C. Section 1734 solely to indicate this fact.

\*\* To whom correspondence should be addressed. Tel.: 81-52-264-4811 (ext. 2088); Fax: 81-561-63-3532; E-mail: kimata@aichi-med-u.ac.jp.

<sup>1</sup> The abbreviations used are: HS, heparan sulfate; FGF, fibroblast growth factor; HGF, hepatocyte growth factor; VEGF, vascular endothelial growth factor; BMP, bone morphogenetic protein; GF, growth factor; HBGF, heparin-binding growth and differentiation factor; CD-SNS, completely desulfated, *N*-sulfated; 2ODS, 2-O-desulfated; 6ODS, 6-O-desulfated; GAG, glycosaminoglycan, IdoUA, L-iduronic acid; HexA, hexuronic acid; GlcNSO<sub>3</sub>, *N*-sulfoglucosamine; HS2ST, heparan sulfate 2-O-sulfotransferase; HS6ST, heparan sulfate 6-O-sulfotransferase; PBS, phosphate-buffered saline; BSA, bovine serum albumin; PAPS, adenosine 3'-phosphate,5'-phosphosulfate; ELISA, enzyme-linked immunosorbent assay; HPLC, high performance liquid chromatography; h, human; Octa, octasaccharide; SPR, surface plasmon resonance.

unique structure. However, our knowledge about the heparin/HS structures involved in the interaction with a variety of HBGFs is still limited, and the greater part of the interactions between HS and the heparin-binding proteins remains to be studied. Furthermore, structural analyses of HS with binding activity for HBGFs often give different results when HS is isolated from different sources (29, 30).

In the present study, we prepared an octasaccharide library consisting of well defined sulfated octasaccharides. The library comprised 2-*O*-sulfated or 6-*O*-sulfated octasaccharides generated from CDSNS-heparin-derived octasaccharide (Octa-I) by *in vitro* reactions with HS2ST or HS6ST. By using this library, we examined the structures that were specifically bound to the various HBGFs including FGF-2, FGF-4, FGF-7, FGF-8, FGF-10, FGF-18, HGF, BMP-6, and VEGF. Our results show that these HBGFs could be classified roughly into five groups on the basis of the difference in affinity with the oligosaccharides, and offer further evidence for specific interactions between heparin-binding growth factors and the corresponding domain structures in HS. Furthermore, for a physiological relevance of this study, we demonstrated specific release of FGF-10 and FGF-2 from HS by the addition of 6-*O*-sulfated Octa-I and 2-*O*-sulfated Octa-I, respectively.

#### EXPERIMENTAL PROCEDURES

**Materials**—Completely desulfated, *N*-sulfated heparin (CDSNS-heparin), chondroitin 4-sulfate from whale cartilage, heparitinase I (*Flavobacterium heparinum*, EC 4.2.2.8), heparitinase II (*F. heparinum*, no number assigned), heparinase (*F. heparinum*, EC 4.2.2.7), 2-*O*-desulfated heparin (2ODS-heparin), 6-*O*-desulfated heparin (6ODS-heparin), and an unsaturated glycosaminoglycan disaccharide kit were obtained from Seikagaku Corp. (Tokyo, Japan). Heparin and unlabeled PAPS were purchased from Sigma. [<sup>35</sup>S]PAPS was purchased from PerkinElmer Life Sciences. [<sup>3</sup>H]NaBH<sub>4</sub> (36 Ci/mmol) was purchased from Amersham Biosciences. Hiloal Superdex 30 HR 16/60, fast desalting column HR 10/10, Mono Q HR 5/5 and PD-10 were from Amersham Biosciences. Senshu Pak Docosil was obtained from Senshu Scientific (Tokyo, Japan). Recombinant human FGF-7, FGF-10, and FGF-18 were provided by Amgen Inc. (Thousand Oaks, CA). Recombinant human FGF-2 was purchased from Progen Biotechnic GmbH (Heidelberg, Germany). Recombinant human FGF-8 was purchased from PeproTech (Rocky Hill, NJ). Recombinant human FGF-4 was purchased from R & D Systems (Minneapolis, MN). Recombinant human HGF was purchased from Genzyme-Technie (Minneapolis, MN). Recombinant bone morphogenetic protein 6 (BMP-6) was a gift from Creative Biomolecules Inc., Hopkinton, MA, courtesy of Dr. T. K. Sampath. Recombinant human VEGF<sub>165</sub> was purchased from Diadone Research (Cedex, France). Sensor chip SA was obtained from BIAcore AB (Uppsala, Sweden).

**Preparation of Octasaccharide Fractions from CDSNS-heparin and Heparin**—One octasaccharide composed of HexA-GlcNSO<sub>3</sub> (Octa-I) and another composed of HexA(2SO<sub>3</sub>)-GlcNSO<sub>3</sub>(6SO<sub>3</sub>) (Octa-II) were prepared from CDSNS-heparin and heparin, respectively, as follows. One hundred milligrams of CDSNS-heparin was digested with 0.1 unit of heparitinase I, which is known to preferentially cleave glucosaminidic linkages to nonsulfated HexA residues in heparin/HS, at 37 °C for 2 h. The unsaturated oligosaccharide products were separated by Superdex 30 chromatography based on size. Octasaccharide fractions were pooled and lyophilized. The lyophilized materials were applied to a Mono Q column. The Mono Q column was developed by using a linear gradient from 0.2 to 1.2 M NaCl in 50 mM glycine-HCl, pH 3.0. The fractions eluted around 0.34 to 0.38 M NaCl were pooled and desalted by PD-10 column chromatography. The purified octasaccharide thus obtained was designated Octa-I. About 250 nmol (as HexA) of Octa-I was obtained. One hundred milligrams of heparin was digested with 0.1 unit of heparinase, which is known to cleave preferentially glucosaminidic linkages to 2-*O*-sulfated IdoUA in heparin/HS, at 37 °C for 2 h. Octa-II was purified from the heparin digests by the methods described above except that the fractions eluted over 1.0 M NaCl were pooled in the Mono Q chromatography. About 2.4 μmol (as HexA) of Octa-II was obtained. Aliquots of Octa-I and Octa-II were reduced with [<sup>3</sup>H]NaBH<sub>4</sub> as described by Shively and Conrad (33). The specific activities of <sup>3</sup>H-labeled Octa-I and Octa-II were 1.5 × 10<sup>4</sup> and 1.2 × 10<sup>4</sup> dpm/nmol, respectively.

**Preparation of *O*-Sulfated CDSNS-Heparin Octasaccharide with Recombinant HS2ST and HS6ST-I**—The recombinant hHS2ST and hHS6ST-1 were prepared and purified as described previously (19). Briefly, FLAG-CMV2-hHS2ST or hHS6ST-1 was transfected into COS-7 cells. After 72 h, the recombinant fusion proteins were extracted from the cell layer with 10 mM Tris-HCl, pH 7.2, 0.5% (v/v) Triton X-100, 0.15 M NaCl, 20% glycerol, 10 mM MgCl<sub>2</sub>, and 2 mM CaCl<sub>2</sub>, and purified with an anti-FLAG M2 antibody-conjugated affinity column.

2-*O*-Sulfated Octa-I and 6-*O*-sulfated Octa-I were prepared as follows. For 2-*O*-sulfation of Octa-I, the reaction mixture contained, in a final volume of 50 μl, 1.0 μmol of acetate buffer, pH 5.5, 3.75 μg of protamine chloride, 0.5 nmol of Octa-I, 1 μCi/2 nmol of [<sup>35</sup>S]PAPS, and 2.7 units of hHS2ST. For 6-*O*-sulfation, the reaction mixture (50 μl) contained 2.5 μmol of imidazole-HCl, pH 6.8, 3.75 μg of protamine chloride, 0.5 nmol of Octa-I, 2 nmol of [<sup>35</sup>S]PAPS (1 μCi), and 5.5 units of hHS6ST-1. After incubation at 37 °C overnight, the reactions were stopped by heating at 100 °C for 1 min. 2-*O*-<sup>35</sup>S-Sulfated Octa-I and 6-*O*-<sup>35</sup>S-sulfated Octa-I were precipitated with 3 volumes of ethanol containing 1.3% potassium acetate and 0.5 mM EDTA in the presence of the carrier chondroitin 4-sulfate (0.1 μmol as glucuronic acid). The precipitates were dissolved in a small volume of distilled water and subjected to Mono Q chromatography. The Mono Q chromatography was developed with a linear gradient from 0.2 to 0.8 M in 50 mM glycine-HCl, pH 3.0.

**Preparation of Growth and Differentiation Factor (HBGF)-conjugated Sepharose Gel**—The growth and differentiation factor-conjugated Sepharose gel was prepared as described previously (30). Briefly, each of FGF-2 (50 μg), FGF-4 (50 μg), FGF-7 (100 μg), FGF-8 (50 μg), FGF-10 (100 μg), FGF-18 (100 μg), HGF (100 μg), BMP-6 (100 μg), and VEGF (50 μg) was coupled to 0.3 ml of CNBr-activated Sepharose 4B gel according to the method recommended by the manufacturer. Acetylated heparin (10 μg) was added to the coupling reaction mixture to protect the heparin/heparan sulfate-binding site of these growth factors.

**HBGF Affinity Chromatography of Various Octasaccharides**—0.1 nmol of <sup>35</sup>S-labeled octasaccharide was dissolved in 0.5 ml of PBST, 0.9 mM CaCl<sub>2</sub>, and 0.2 mg/ml chondroitin 4-sulfate (Binding buffer) and applied to a syringe column of GF-Sepharose (0.3 ml) equilibrated with Binding buffer at 4 °C. The column was shaken gently for 1 h and then washed with 2.5 ml of PBS containing 0.9 mM CaCl<sub>2</sub> and 0.05% Tween 20 (PBST(+)). The column was eluted stepwise with 1 ml of 0.20, 0.25, 0.30, 0.35, 0.40, 0.45, and 0.50 M NaCl in PBST(+) and 2 ml of 2 M NaCl in PBS containing 0.05% Tween 20 (PBST) (Elution buffer). In some cases, the octasaccharides were eluted with 2 ml of Elution buffer after the wash with 2.5 ml of PBST(+). The elution profiles were monitored by measuring the radioactivity in a liquid scintillation counter (30).

**Surface Plasmon Resonance Analysis**—Real time analysis of the interaction of growth factors and heparin/modified heparin was performed with a BIAcore 2000 SPR biosensor. Streptavidin-conjugated Sensor Chip SA was used to immobilize various glycosaminoglycans. Glycosaminoglycans were biotinylated according to the method recommended by the manufacturer. Two hundred micrograms of heparin, 2ODS-heparin, 6ODS-heparin, or chondroitin 4-sulfate was incubated with 74 μg of NHS-LS-Biotin (Pierce) in 100 μl of 50 mM sodium bicarbonate buffer, pH 8.5, for 30 min at room temperature. Biotinylated glycosaminoglycans were precipitated with 2.5 volumes of 95% (v/v) ethanol containing 1.3% (w/v) potassium acetate, and the process was repeated three times. In order to immobilize GAGs on the sensor chip SA, 0.5–2 μg/ml biotinylated GAGs in PBST were injected at a flow rate of 5 μl/min. The injection of biotinylated GAGs produced 10–200 response units of immobilized GAG on the biosensor surface. The amount of bound material on the biosensor chips was measured in arbitrary response units. All measurements were carried out at room temperature, and refractive index errors due to bulk solvent effects were corrected by subtracting away responses on the non-coated sensor chip for GF concentrations used. Each GF stock solutions were diluted with PBST.

Various concentrations of growth factors were injected across the GAG-coated surface at a flow rate of 5 μl/min. The steady state binding level was monitored for 300 s. Sensorgrams were evaluated using BIAevaluation software. Dissociation constants (*K<sub>D</sub>*) for binding could be extracted from the dependence of steady state binding levels on GF concentration. In a steady state, this model calculates *K<sub>D</sub>* from a plot of *R<sub>eq</sub>* against *C* according to the equation, *K<sub>D</sub>* = *R<sub>eq</sub>*(*R<sub>max</sub>* - *R<sub>eq</sub>*)/*C*, where *R<sub>eq</sub>* is the steady state response level for the growth factor; *R<sub>max</sub>* is the maximal capacity of the sensor chip to bind growth factors expressed in response units; and *C* is the molar concentration of growth factor.

**HBGF-releasing Activity of Octasaccharides from HS**—The releasing

TABLE I  
Disaccharide compositions of octasaccharides

The samples were digested with a mixture of heparitinase I and II and heparinase. The products were determined by a reversed-phase ion-pair chromatography with sensitive and specific postcolumn detection. ND, not detected.

Disaccharide component	Octasaccharide library							
	Octa-I	Octa-II	2S-1	2S-2	2S-3	6S-1	6S-2	6S-3
	units/octasaccharide							
HexA-GlcNAc	ND	0.1	ND	ND	ND	ND	ND	ND
HexA-GlcNS	4.0	0.1	2.9	1.9	1.1	2.9	1.9	1.2
HexA-GlcNAc(6S)	ND	0.1	ND	ND	ND	ND	ND	ND
HexA(2S)-GlcNS	ND	0.3	1.1	2.1	2.9	ND	ND	ND
HexA-GlcNS(6S)	ND	0.5	ND	ND	ND	1.1	2.1	2.8
HexA(2S)-GlcNS(6S)	ND	2.9	ND	ND	ND	ND	ND	ND
Yield (%)			40	16	6	38	20	8

activity was measured by ELISA as described previously with a minor modification (30). A 96-well streptavidin-coated plate (Thermo Lab-systems, Finland) was coated with 0.1 nmol (as hexuronic acid) of biotinylated pig aorta HS for 1 h at room temperature. Wells were washed three times with 200  $\mu$ l of PBS and then blocked with 200  $\mu$ l of PBS containing 10 mg/ml BSA for 1 h with gentle shaking. Wells were washed three times with PBS. Then 100  $\mu$ l of Binding buffer (see above) containing 40 ng/ml digoxigenin-conjugated HBGF and 10 mg/ml BSA was added into each well. After 1 h at room temperature, unbound digoxigenin-conjugated HBGF was removed by three washes with PBST(+). Then 100  $\mu$ l of Binding buffer containing 10 mg/ml BSA and 1 pmol to 1 nmol of each octasaccharide were added into the wells. After 1 h at room temperature, wells were washed, and then alkaline phosphatase-conjugated Fab fragments of anti-digoxigenin antibody (1:1000 dilution) were added. After 1 h at room temperature, unbound Fab fragments were removed by three washes with PBST, and the alkaline phosphatase substrate (1 mg/ml *p*-nitrophenyl phosphate in 1 M diethanolamine, pH 9.8) was added into each well. The enzyme activity in each well was measured by using a microplate reader. The experiments were independently repeated three times, and statistical analyses were performed using Student's *t* test. The criterion of significance was shown by *p* values.

**Compositional Analysis of Octasaccharides**—About 0.3 nmol of octasaccharides was digested with a mixture of 1 milliunit of heparitinase I, 0.1 milliunit of heparitinase II, and 1 milliunit of heparinase in 50  $\mu$ l of 50 mM Tris-HCl, pH 7.2, 1 mM CaCl<sub>2</sub>, and 5  $\mu$ g of BSA at 37 °C for 1 h. Unsaturated disaccharide products were analyzed by fluorometric post-column high performance liquid chromatography (HPLC) as reported previously (35).

## RESULTS

**Preparation of an Octasaccharide Library**—Octa-I, an oligosaccharide composed of HexA-GlcNSO<sub>3</sub>, and Octa-II, an oligosaccharide composed of HexA(2SO<sub>4</sub>)-GlcNSO<sub>3</sub>(6SO<sub>4</sub>), were prepared from CDSNS-heparin and heparin, respectively, as described under "Experimental Procedures." The structures of these oligosaccharides were confirmed by digestion with a mixture of heparitinase and heparinase followed by HPLC analysis as described under "Experimental Procedures." As shown in Table I,  $\Delta$ HexA-GlcNSO<sub>3</sub> was exclusively obtained from Octa-I, indicating that the structure of Octa-I was  $\Delta$ HexA-GlcNSO<sub>3</sub>-<sub>3</sub> (HexA-GlcNSO<sub>3</sub>)<sub>3</sub>. On the other hand, 3 mol of HexA(2SO<sub>4</sub>)-GlcNSO<sub>3</sub>(6SO<sub>4</sub>), 0.5 mol of HexA-GlcNSO<sub>3</sub>(6SO<sub>4</sub>), and 0.5 mol of other disaccharide components were released from 1 mol of Octa-II. Octa-II was thus a mixture containing 3 units of HexA(2SO<sub>4</sub>)-GlcNSO<sub>3</sub>(6SO<sub>4</sub>) per molecule.

2-*O*-Sulfated and 6-*O*-sulfated Octa-I were prepared by incubating Octa-I with the recombinant HS2ST and HS6ST-1, respectively, together with PAPS as described under "Experimental Procedures." The *in vitro* sulfated products were separated with Mono Q chromatography (Fig. 1). Both 2-*O*-sulfated Octa-I and 6-*O*-sulfated Octa-I were separated into three peaks: 2S-1, 2S-2, and 2S-3 for 2-*O*-sulfated Octa-I; and 6S-1, 6S-2, and 6S-3 for 6-*O*-sulfated Octa-I. All of these peaks were eluted at higher NaCl concentration than Octa-I and at lower NaCl concentration than Octa-II. Each peak was pooled sepa-

rately. To examine the structure of these products, aliquots of these sulfated octasaccharides were digested extensively with the mixture of heparitinase and heparinase and subjected to HPLC as described under "Experimental Procedures." From the disaccharide compositions shown in Table I, it is evident that 2S-1, 2S-2, and 2S-3 contained 1, 2, and 3 units, respectively, of the HexA(2SO<sub>4</sub>)-GlcNSO<sub>3</sub> component; and 6S-1, 6S-2, and 6S-3 have 1, 2, and 3 units, respectively, of HexA-GlcNSO<sub>3</sub>(6SO<sub>4</sub>) component. Under the maximum reaction conditions used, more than 60% of Octa-I was sulfated by each sulfotransferase. The yields of these sulfated Octa-I were decreased as the content of 2-*O*-sulfated or 6-*O*-sulfate units was increased (Table I).

**Binding Abilities of Octa-I and Octa-II to Various HBGFs**—Before determining the binding activity of oligosaccharides, we examined the binding ability and capacity of the growth and differentiation factor-conjugated Sepharose 4B affinity columns using <sup>3</sup>H-labeled heparin (2 nmol as HexA). Every affinity column conjugated with FGF-2, FGF-4, FGF-7, FGF-8, FGF-10, FGF-18, HGF, VEGF, or BMP-6 bound more than 80% of the applied <sup>3</sup>H-labeled heparin (data not shown). To examine the binding activity of the oligosaccharide libraries synthesized enzymatically, we first applied [<sup>3</sup>H]NaBH<sub>4</sub>-reduced Octa-II (0.5 nmol as octasaccharide) to the growth factor-conjugated columns. The amounts of Octa-II bound to various growth factor-conjugated columns are shown in Fig. 2. FGF-2, FGF-4, FGF-18, and HGF bound Octa-II strongly. FGF-10 and FGF-7 also bound Octa-II slightly weaker than FGF-2. In contrast, FGF-8, BMP-6, and VEGF hardly bound Octa-II (less than 15% of the applied). These results indicate that FGF-2, FGF-4, FGF-7, FGF-10, FGF-18, and HGF have high affinity to Octa-II as observed for heparin, but FGF-8, BMP-6, and VEGF have very weak or no affinity to Octa-II, although these proteins showed high affinity to heparin. The results suggest that oligosaccharides longer than octasaccharides may be required for the binding of FGF-8, BMP-6, or VEGF.

Octa-II contains both *O*-sulfate and *N*-sulfate. To address which sulfate groups are necessary for the binding to these growth factors, we examined the binding of Octa-I which is devoid of *O*-sulfate but has *N*-sulfate. As shown in Fig. 2, Octa-I hardly bound at all to the growth factor-conjugated affinity columns (*open bars* in Fig. 2). These results clearly indicate that the *O*-sulfate groups in Octa-II are essential for the binding to these growth factors.

**Affinity of the Octasaccharide Library to Various HBGFs**—Octa-II is composed of 3 units of HexA(2SO<sub>4</sub>)-GlcNSO<sub>3</sub>(6SO<sub>4</sub>). To determine whether either or both of the 2-*O*-sulfate and 6-*O*-sulfate groups interact with the growth factors, we examined the binding of 2-*O*-sulfated or 6-*O*-sulfated Octa-I to the growth factor-conjugated columns that could retain Octa-II. In Fig. 3, the binding of 2S-3 and 6S-3 to FGF-2, FGF-4, FGF-7,

FIG. 1. Mono Q column chromatography of 2-O-sulfated Octa-I and 6-O-sulfated Octa-I generated *in vitro* by recombinant enzymes. 10 nmol of Octa-I was incubated with 20  $\mu$ Ci/40 nmol of [<sup>35</sup>S]PAPS and recombinant human HS2ST or recombinant human HS6ST-1 overnight. 2-O-Sulfated Octa-I (A) and 6-O-sulfated Octa-I (B) were applied to a Mono Q column and eluted as described under "Experimental Procedures." Aliquots of fractions served for the measurements of radioactivity. The fractions shown by solid horizontal bars were pooled and desalted for analysis. Broken lines represent the concentration of NaCl. Arrows indicate the elution position of Octa-I. Insets show the elution profiles of the reaction products after the incubation for 90 min.

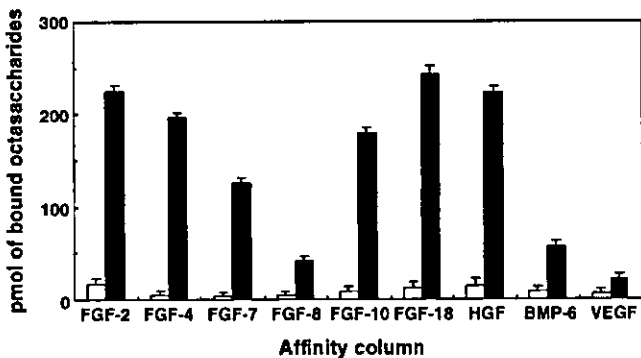
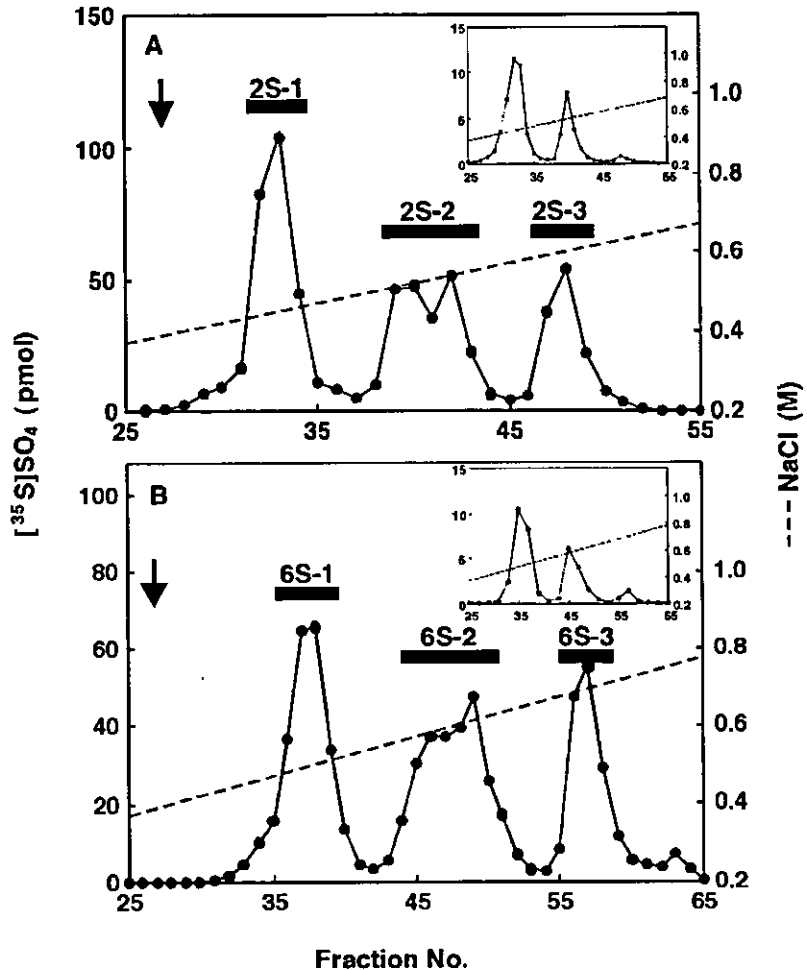


FIG. 2. Binding of Octa-I and Octa-II to various growth and differentiation factors. 500 pmol of <sup>3</sup>H-labeled Octa-I and Octa-II was applied to the GF affinity column as described under "Experimental Procedures." After incubation at 4 °C for 1 h, the column was washed with Binding buffer and then eluted with Elution buffer (bound fraction). Open bars and closed bars indicate amount of bound Octa-I and Octa-II, respectively.

FGF-10, FGF-18, or HGF-conjugated columns is shown. FGF-2 bound 2S-3 strongly but did not bind 6S-3. These results are consistent with studies showing that the presence of 1 unit of the HexA(2SO<sub>4</sub>)-GlcNSO<sub>3</sub> component in oligosaccharides is sufficient for the binding to FGF-2 (26, 27). In contrast, FGF-10 interacted moderately with 6S-3 but little with 2S-3. FGF-18 and HGF bound both 2S-3 and 6S-3, but preferred 2-O-sulfated to 6-O-sulfated octasaccharides. Because FGF-4 and FGF-7 bound neither 2S-3 nor 6S-3, these HBGFs appear to require trisulfated disaccharide units, IdoUA(2SO<sub>4</sub>)-GlcNSO<sub>3</sub>(6SO<sub>4</sub>), for the binding of oligosaccharides. Alternatively, FGF-4 and

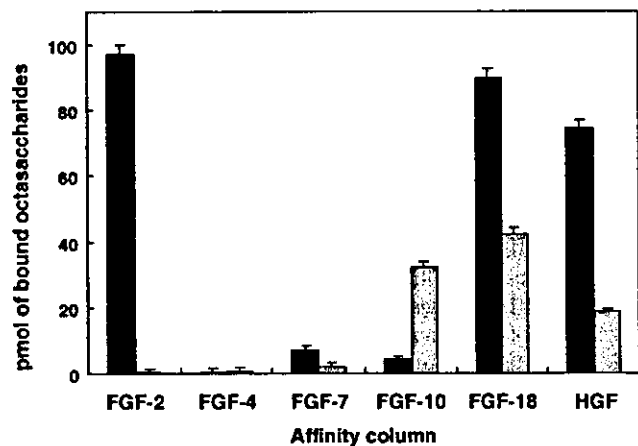


FIG. 3. Binding of 2S-3 and 6S-3 to various growth and differentiation factors. 100 pmol of octasaccharides "2S-3" and "6S-3" was subjected to the GF affinity column chromatography as described under "Experimental Procedures." After incubation at 4 °C for 1 h, the column was washed with Binding buffer and then eluted with Elution buffer (bound fraction). Closed bars and gray bars indicate amount of bound 2S-3 and 6S-3, respectively.

FGF-7 may bind octasaccharides containing both IdoUA(2SO<sub>4</sub>)-GlcNSO<sub>3</sub> and HexA-GlcNSO<sub>3</sub>(6SO<sub>4</sub>) units. These results suggest that each growth factor may recognize the characteristic sulfation pattern of the octasaccharides. Furthermore, we determined the effect of the number of sulfate groups attached to the octasaccharides on the binding to HBGFs using octasaccharides with one, two, or three 2-O-sulfate groups (2S-1, 2S-2, and 2S-3) and octasaccharides with